Towards an Intelligent Bed Sensor: Non-intrusive Monitoring of Sleep Disturbances via Computer Vision Techniques

by

Kaveh Malakuti

BSc, Azad University, 2004
MSc, Shahid Beheshti University, 2006
MASc, University of Victoria, 2008

A Thesis Submitted in Partial Fulfillment of the
Requirements for the Degree of

Master of Applied Science

in the Department of Electrical and Computer Engineering

University of Victoria

Towards an Intelligent Bed Sensor: Non-intrusive Monitoring of Sleep Disturbances via Computer Vision Techniques

by

Kaveh Malakuti

BSc, Azad University, 2004
MSc, Shahid Beheshti University, 2006

Supervisory Committee

Dr. A. Branzan Albu, Co-Supervisor (Department of Electrical and Computer Engineering)

Dr. T. Darcie, Co-Supervisor (Department of Electrical and Computer Engineering)

Dr. M. Sima , Departmental Member (Department of Electrical and Computer Engineering)

Supervisory Committee

Dr. A. Branzan Albu, Co-Supervisor (Department of Electrical and Computer Engineering)

Dr. T. Darcie, Co-Supervisor (Department of Electrical and Computer Engineering)

Dr. M. Sima , Departmental Member (Department of Electrical and Computer Engineering)

Abstract

Sleep related breathing irregularities and sleep disturbances affect a surprisingly large number of people in the society. Due to the high risks of chronic and acute health situations associated with sleep disturbances, a robust sleep monitoring system is needed. While the current golden standard for sleep monitoring is the Polysomnograph (PSG), other approaches also require attachments to patients' body. Furthermore, these monitoring techniques are performed in sleep clinics. Therefore, they interfere with natural sleep patterns. Finally these techniques are usually expensive. The Intelligent Bed Sensor is proposed as a non-restraining home-based sleep monitoring system. It uses 144 pressure sensors embedded in a bed sheet for measuring the pressure that the patient's body exerts on the bed. The main theoretical contribution of this work is a new methodology for analyzing periodicity in pressure data via Computer Vision techniques. We prove that the Intelligent Bed Sensor is capable of detecting individual respiration cycles, apnea events and movements accurately.

Table of Contents

List of Figures

List of Tables

List of Algorithms

Acknowledgements

I would like to express my deepest gratitude, first and foremost, to my supervisors, Dr. Alexandra Branzan Albu and Dr. Thomas E. Darcie for their support, help and guidance from the very first stages of my studies until the last. I also extend my appreciation to Dr. Albu for the valuable knowledge I have gained during the interdisciplinary team works with experts from Psychology, Centre on Aging, Ergonomics, Software Engineering and Computer Science. I do not think I would have found this path without her generous help.

My Master's studies were supported in part by MITACS and Vigil Health Solutions. I also thank Steven Smith from Vigil Health Solutions and David Lokhorst and Joshua Hayes from Tactex Controls for their technical support and providing the bed sensor used in this study.

I want to acknowledge volunteers who generously helped in creating the database for this study. I also thank Dr. Jens Weber-Jahnke and his team for sharing their research lab space willingly during my experiments.

I cannot end without thanking my family and Nasim Abedi, for being patient and supportive of my studies away from home. I could not have achieved so far without their moral support.

Kaveh Malakuti, Victoria, British Columbia, Canada

Dedication

To my father, Abbas Malakuti,

my mother, Azam Najafian,

my sister, Gelareh Malakuti

and Nasim Abedi.

Chapter 1

Introduction

According to clinical research, to completely restore mental alertness and physical wellbeing, most adults require an average of eight hours of sleep a night [9]. Sleep deprivation is a subjective assessment based on the individuals degree of day time sleepiness and alertness. Therefore, it is not only related to quantity but also the quality of sleep. Even sleep disruption without evidence of arousal results in increased objective daytime sleepiness and mood alterations [37]. Therefore, sleep disorders such as sleep apnea, which cause significant sleep fragmentation, result in severe sleep-deprivation, lowering the patients quality of life and work performance.

Factors that affect the sleep quality and quantity are circadian rhythm disturbances (due to occupation or academic demands), poor sleep ambiance (such as hospital setting), and sleep disorders. All of these lead to excess daytime sleepiness, fatigue, and inattention, in turn interfering with individuals optimal performance at work, school, and on the roads. For example, in United States two in five adults sleep less than 7 hours each weeknight, and three in eight believe that their sleepiness during the day interferes with their daily activities at least a few times a month [60]. Strikingly due to increased demands of our modern societies, the proportion of adults

in the United States sleeping less than seven hours per night has increased from 16 to 37 percent over the past 40 years [75].

Sleep disorders are common causes of sleep deprivation. For example, a study indicates that in Japan the quota for sleep dissatisfaction is 50% in adults. 25 million of Japanese suffer from some kind of sleep disorder and 40% of this group have a form of Sleep Disordered Breathing (SDB) such as Sleep Apnea Syndrome (SAS) [65]. Sleep disorders cause disrupted nocturnal sleep and thus daytime hyper-somnolence, which leads to impaired alertness and performance, increasing the risk of sleep related motor vehicle accidents and occupational injury. In fact, excessive sleepiness is the second leading cause of car accidents and a major cause of truck accidents in the United States [40, 48]. Studies have shown that drivers with sleep-related breathing disorders perform poorly on several types of driving simulators and have an automobile crash rate greater than other drivers [53] . For example, among patients with severe sleep apnea, the incidence of sleep-related motor vehicle crashes was found to be nearly twice that of patients with mild or moderate sleep apnea. Another study done in Switzerland found that patients with moderate to severe Sleep Apnea Syndrome (SAS) have up to fifteen fold increase risk of motor vehicle accidents (MVA), which can be reduced with adequate treatment (the MVA rates dropped from 10.6 to 2.7 per million km ($p \leq 0.5$) after treatment with nasal continuous airway pressure (nCPAP)) [27].

Sleep deprivation has other adverse consequences besides fatigue and impaired alertness. It can result in cognitive deficits, changes in mental status, and measurable neuropsychological deficits [33]. Sleep deprivation has also been reported to change the respiratory physiology. It depresses the ventilatory responses to hypercapnia (high carbon dioxide levels) and hypoxia (low oxygen levels) leading to hypoventilation in an individual's such as in hospitalized patients [71] . It also decreases respiratory muscle endurance and thus it can affect exercise capacity [15].

Perhaps one of the most adverse consequences is the immuno-suppressive effects of sleep deprivation. For example, complete sleep deprivation of rats for several weeks results in their death due to severe infection resulting from breakdown of their defense systems [20]. In humans, partial or total sleep deprivation results in increase production of pro-inflammatory proteins, as is seen with an infection [69].

Sleep deprivation also affects appetite with negative metabolic consequences. This was illustrated in a study of 12 healthy, normal weight, adult men who underwent two nights of sleep restriction and two nights of sleep extension in a randomized order, spaced six weeks apart with controlled conditions of caloric intake and physical activity [59]. Sleep restriction, when compared to sleep extension, was associated with a decrease in serum leptin (appetite suppressing hormone), an increase in serum ghrelin (an appetite promoting hormone), and increased hunger and appetite (in particular for calorie-dense foods with high carbohydrate content).

Sleep-disordered breathing is a group of sleep disorders characterized by an abnormal respiratory pattern (such as apneas, hypoapneas, or respiratory effort related arousals) or an abnormal reduction in gas exchange (ie, hypoventilation) during sleep. These events can produce arousals from sleep, increase arterial carbon dioxide, or decrease oxygen levels. Therefore, it causes sleep deprivation and alters sleep architecture, resulting in daytime symptoms and organ/system dysfunction. Several types of apneas may be observed during sleep. These include obstructive apnea, central apnea, mixed apnea, and hypo-apnea. An obstructive apnea occurs when airflow is absent or nearly absent, but ventilatory effort persists. It is caused by complete, or near complete, upper airway obstruction or collapse, often accompanied by snoring and inspiratory flow cessation. Central apnea occurs when both airflow and ventilatory effort are absent and are due to decrease inspiratory effort. Mixed apnea is when central apnea pattern usually precedes an obstructive apnea pattern. Hypopneais a reduction of airflow to a degree that is insufficient to meet the criteria for an

apnea [29]. Obstructive sleep apnea-hypopnea (OSAH) is very common and affects 24 and 9% of middle-aged men and women, respectively. In some populations at risk, the prevalence of OSA may even reach 50%. It OSAH is often due to reduced upper airway caliber due to excess surrounding tissue or very compliant airway. It is defined as either more than 15 apneas, hypopneas, or respiratory effort related arousals (RERAs) per hour of sleep in an asymptomatic patient or more than 5 apneas, hypopneas, or RERAs per hour of sleep in a patient with symptoms of signs of disrupted sleep (snoring, restless sleep, breathing pauses) [61]. The repeated apnea episodes result in frequent arousals and sleep fragmentation, diminishing the quality and quantity of sleep.

In addition to the above mentioned consequences of sleep deprivation, obstructive sleep apnea poses a number of cardiovascular risks to the patient [22, 73]. These include systemic hypertension, pulmonary hypertension, coronary artery disease, and cardiac arrhythmia.

Given its many detrimental health effects and its high prevalence, apnea poses great cost to individual and the society. However, since effective treatment of apnea can reverse most of its harmful cardio-pulmonary side effects as well as eliminate sleep deprivation and its consequences, early detection is of enormous value, decreasing the associated health care and other costs to society and improving individuals quality of life. Therefore, we propose the intelligent bed sensor, a novel computer vision based approach for monitoring sleep. Our system uses affordable sensors that can be installed on all kinds of mattresses. Its low cost, easy installation and maintenance-free design, makes the intelligent bed sensor an affordable home-based sleep monitoring system.

In the following chapters, we will first review the past and current standards and trends in sleep monitoring. The intelligent bed sensor is proposed in chapter 3. Chapter 4 includes the experimental results and discussion. Finally, chapter 5 draws

conclusions and outlines future work to improve the performance of the intelligent bed sensor.

Chapter 2

Related Work

2.1 Introduction

Potential health risks associated with sleep disordered breathing syndrome necessitates a reliable nocturnal sleep monitoring system. Researchers have been studying various techniques for detection and classification of respiration and other biophysiological signals for the purpose of sleep monitoring. These approaches can be categorized as intrusive or non-intrusive. Intrusive techniques are those that require sensors be attached to or worn by human subject. Non-intrusive techniques, on the other hand, embed sensors in the monitoring environment (for example in the bed). The rest of this section reviews past and current trends in sleep monitoring using both categories of approaches.

2.2 Approaches based on sensors attached to/worn by the human subject

Also known as intrusive monitoring, these techniques require sensors that are attached to subject's body. They usually restrain natural motion. For the most part,

intrusive approaches show better results compared to non-intrusive approaches. This is, in fact, due to the direct contact and more accurate measurements by attached sensors. Accuracy, however, is achieved by sacrificing subject comfort. This also interferes with subject's natural sleep patterns. In addition, these techniques are usually expensive. Hence, longer durations of monitoring are typically costly and hard to achieve compared to non-intrusive techniques.

2.2.1 Polysomnography

The current widely accepted standard for monitoring nocturnal sleep is Polysomnography (PSG). It measures and records bio-physiological signals including Electrooculogram (EOG), Electroencephalogram (EEG), Electrocardiogram(ECG or EKG), Electromyogram (EMG), breathing or respiratory efforts, abdominal and thoracic movements during sleep [26]. Accurate assessment of sleep quality is achievable by means of analyzing PSG recordings. However, its relatively high cost makes it impractical for long-term sleep monitoring. Besides, it is considered an intrusive method as so many sensors are attached to the subjects body. It can disturb the patients natural sleep, so the measured data may not accurately represent patients actual sleep behavior [49]. Beside assessment of PSG recordings by health specialists, automatic techniques have been developed by researchers in order to detect and characterize respiration patterns and sleep disturbances. Such techniques either employ all information sources available in the PSG recordings, for example, [68], or use one or more data channels in the PSG recording. In [68], the authors have used the whole PSG recording and four Artificial Neural Networks in order to classify data into phases of normal breathing, hypoapnea and apnea. Among approaches that process one or more channel of PSG data, the majority of them particularly work on electrical activity of the heart during PSG.

ECG based techniques

Electrical activity of the heart is known to have justified relation to sleep phases [72]. Therefore, one of the most important signals captured during PSG is the ECG. The simplest feature to extract from an ECG time series is the heart rate. The standard for calculation of heart rate is the R-R interval (RRI) or the interval between the highest peaks of two consecutive cardiac cycles, as shown in figure 2.1. The RRI was shown to be a robust measure for the hear rate [18, 28]. Hilbert transform has also been applied to ECG signals, [62, 63], to extract QRS complex, which is another unique feature in each cardiac cycle and could be utilized for heart rate determination.

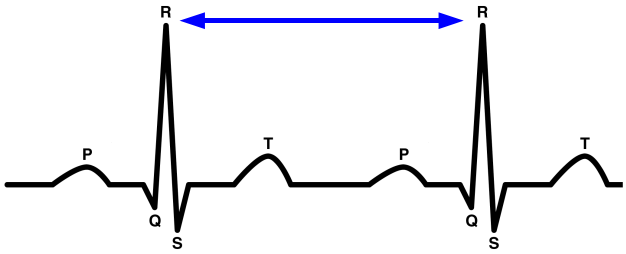

Figure 2.1: The QRS complex and R-R interval

Variability of heart rate could be used as an indication of sleep stage and sleep disorders. Heart rate variability (HRV) is sensitive to both Rapid Eye Movement (REM) sleep and apnea [63]. Consequently, another source of information is required to distinguish between REM sleep and apnea event. R-wave attenuation is used as the complementary source of information along HRV in [62, 63]. HRV is both processed in both time [62] and frequency [63] domains.

Respiration was derived from ECG using Wavelet Transforms [74] and other signal processing techniques [13]. Apnea could also be extracted directly from surface ECG signals [39] by means of Autoregressive models. Furthermore, combination of ECG and other sources such as Arterial Blood Pressure (ABP) [28], Inducted Plethysmography [43], Peripheral Arterial Tonometry (PAT), Oximetry, and EMG [50],

phase/time delay between ECG and other bio-signals [21] for the purpose of sleep monitoring and apnea detection has also been investigated.

Blood Oxygen Saturation

Saturation of oxygen in Blood (SaO2 or SpO2) changes regularly as a result of respiration. SaO2 is also one of the signals that are gathered during PSG. SaO2 could be used for detection of apnea if processed separately, by means of central tendency measures [36] or adjoint with other signals, such as measurement of airflow in upper airways, as in [57], or PAT, ECG and EMG, as in [50]. The correlation between airflow and oxygen saturation was investigated in [57] for detection of obstructive sleep apnea. Peripheral arterial vascular tone measured using a plethysmographic method on the finger was used in [50] for detection of sleep-related breathing irregularities. Figure 2.2 clearly shows considerable decline in the level of SaO2 during events of obstructive sleep apnea.

2.2.2 Actigraph

Another widely used recording device is The Actigraph, also known as an activity monitor. Actigraph is a wrist-watch like device that uses internal accelerometers to detect activity by sensing motion. This small lightweight activity-measuring instrument can be worn on the wrist, waist, or ankle to record physical activity [55]. It has been used in various studies in the field of sleep monitoring: [4–6]. Actigraph has certain advantages over PSG although only one physiological variable(in other words, limb motion) is measured. The most important of all is that sleep and wake state information could be recorded continuously for much longer durations in comparison with PSG, in other words, weeks or even longer. Hence it facilitates long-term sleep-monitoring.

Nevertheless, Actigraph has the same disadvantage of PSG. Although patient's com-

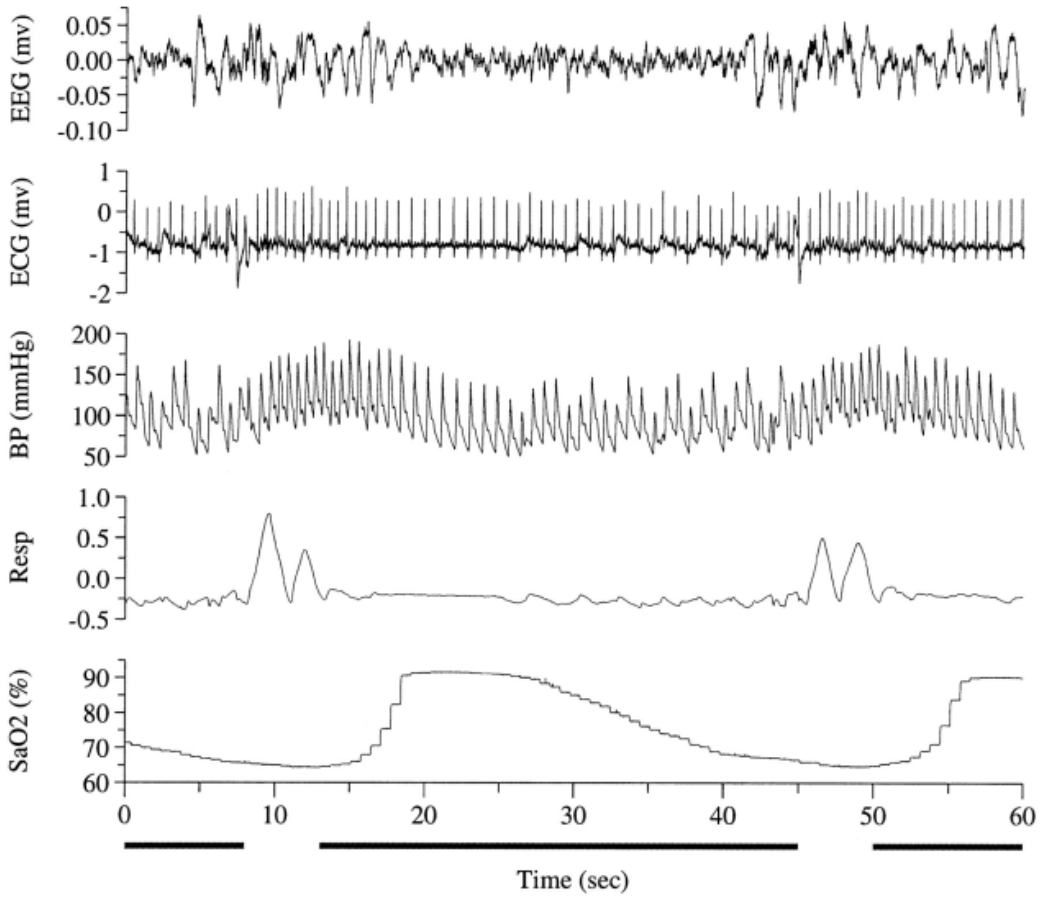

Figure 2.2: Changes in SaO2 level, cardiopulmonary and electroencephalographic (EEG) dynamics during two obstructive sleep apnea events. (image courtesy of physionet.org)

fort is much more in actigraphy compared to PSG, the device is still intrusive. Some people may find wearing a wrist-watch type device during sleep uncomfortable. Besides, the devices are still relatively expensive (more than $1000). Above all, the main drawback to actigraphy is that it is less useful in detecting disorders when limb motion is not involved, for example, Apnea, [54].

Like previously discussed sources of information, actigraph could also be processed in conjunction with other sources such as PAT [2], Oximetry, ECG, EMG [50] for the purpose of sleep monitoring and particularly, obstructive apnea detection.

2.2.3 Bio-shirts

A recent trend in sleep monitoring that also has a tendency toward non-intrusive monitoring systems is the bio-shirt, also known as life-shirt. Bio-shirts measure a set of physiological parametes including ECG, skin temperature, respiration derived from Inductive Plethysmography (IP) and acceleration along two axes [43].
The patient wears the bio-shirt, as shown in figure 2.3. The shirt transmits measured values to a computer system for further analysis. This method has recently been shown to have comparable accuracy to PSG in sleep monitoring and apnea detection [25] in a sleep lab environment.

Figure 2.3: Left: bio-shirt inner layer. Right: outer layer. (Picture from [43])

2.2.4 Approaches using Strain Gauge

Respiration is carried out by muscles moving the rib cage, consequently changing the pulmonary volume and creating pressure changes needed to cause the airflow. Thus, physical movement is essential in respiration. There are techniques which concentrate on ribcage and abdominal movements in order to extract information about respiration cycles, apnea events and their type (Central vs. Obstructive). Varady and Bongar in [66] have been able to extract apnea events, their type and grade using phase relation information between abdominal and thoracic respiration movement signals. It is known that in a normal breathing pattern, the phase difference

between aforementioned two signals is zero. However, depending on the degree of airway obstruction, the phase difference increases [66]. This method was shown to have overall 90% accuracy compared to reference annotations made by medical experts. The type of apnea could trivially be detected: in central apnea, no or only very small movement is recorded, while in obstructive type, movements are recorded, but with different phases [67].

In another study, [52], Fuzzy Logic algorithms were applied to abdominal respiration movements measured by a strain gauge. Abdominal movements cause changes in electrical resistance of the strain gauge, the electrical signal is amplified, filtered, digitized and transmitted to a computer for processing. Autoregressive and modified zero-crossing models have been used to classify respiration episodes as normal or respiration with artifact, for example, apnea.

2.2.5 Other approaches

Beside signal sources discussed earlier, researchers have been using sound, pressure and optical signals as well. In [32], the authors placed a sensitive microphone on patients' chest in an area close to the heart, thus picked up respiration, cardiac and snoring sounds for analysis and detection of apnea and its type.

Airway pressure signals measured by constant positive airway pressure (CPAP) devices were used in combination with SaO2 signals for detection of apnea in [57]. Salisbury and Sun, have been able to extract Obstructive Sleep Apnea (OSA) by means of nonlinear and nonstationary signal processing algorithms applied to nasal airway pressure data [56].

Arterial Blood Pressure (ABP) and central venous pressure wave forms have been processed by an Independent Component Analysis (ICA) based algorithm to extract respiration in [58]. Alternatively, ABP, HR and R-R intervals were first processed by three algorithmic models: additive, amplitude modulation and frequency modula-

tion. A linear estimator was applied to the results to extract respiration [28]. Finally, photoplethysmographs were used in [23] for the same purpose.

2.3 Approaches based on sensors embedded in environment

Measurements done in these approaches do not require direct contact or attachments to patients' body; therefore, they are considered to have minimal or no interference with the patients' natural sleep patterns. Unlike intrusive approaches, these methods measure environmental changes induced by the patients sleep related physiological functions. We may classify these non-intrusive approaches according to the type of sensors used, as follows:

(A) approaches using Acoustic Sensors,

(B) approaches using Multi-modality sensors,

(C) approaches using Pressure Sensors,

(D) Vision Based approaches.

A brief survey covering the 4 classes follows. (A) A capacitor based acoustic sensor (microphone) is enclosed in an air pillow and placed under subject's occiput in [38]. The acoustic signals from the microphone are amplified, digitized and sent to a computer workstation for processing. By applying Kalman filters and the maximum likelihood method to dynamic models of heartbeat and respiration, instantaneous periods of heartbeat and respiration are extracted. Matsubara et al. ([38]) have adopted one common band pass filter to extract the heartbeat and respiration signals simultaneously, and proposed use of a common dynamic model to measure the heartbeat and respiration periods. Although they have achieved reasonable accuracy

in detecting respiration and heartbeat periods, their method is quite vulnerable to acoustic noises. An example of such noise would be snoring, which is common among patients suffering from SDB.

Some researchers have developed systems to employ multiple sensors for monitoring patients during sleep. For instance, Peng et al. [49] use video cameras, passive infrared sensors and heart rate sensors as sources of information. They apply machine learning algorithms to motion information from multiple sensors for determination of sleep / wake state. Their approach shows comparable results with actigraphy.

Other examples of approaches based on multi-modality sensors are [45] and [44]. Nishida et al. use the combination of 221 pressure sensors that are 5 cm apart from each other, 6 CCD cameras and 2 microphones on the ceiling as information sources [45]. Their "human symbiosis" system was designed to monitor respiration and posture on the bed without involving health care professionals. The "human symbiosis" system was shown to be able to operate over extended durations (over 6 hours). In order to detect respiration, they select a reference pressure sensor that has the largest power spectrum between 0.25Hz and 0.33Hz. The rest of the 220 pressure sensors are classified into two classes according to their phase difference with the reference sensor. Finally respiration is derived by subtracting the sum of pressure values of each class. This method was shown to be effective for detecting respiration while the subject is in supine, lateral and prone postures.

Another similar approach, which is based on sensorizing the furniture is [44]. It uses 210 pressure sensors, one dome microphone on the ceiling and a washstand display. The pressure sensors are sources of information for respiration and posture detection, the microphone picks up the breathing sounds and the display shows information to the patient. This system is able to monitor respiration and detect obstructive apnea events.

Studies that use pressure sensors as the only source of information can be further

categorized into two subcategories: those that use direct pressure induced on the pressure sensors and approaches that use changes in the pressure of the mattress or the pillow. Approaches in the first subcategory use pressure sensitive films. These films are either Piezo electric [12] or Electromechanical Film sensors (EMFi) [51].

In [12], the authors used a Piezo film made of aluminum nitride (AlN) as the pressure sensor sheet and applied Empirical Mode Decomposition (EMD) on the pressure values to detect respiration and heart beat. Similarly, an Electromechanical Film (EMFi) was used in [51] as the pressure sensor sheet. Postolache et al. ([51]) applied discrete wavelet transform to decompose pressure signals. Later stationary wavelet transformation was used for filtering the data. They have been able to detect respiration and Ballistocardiogram (BCG).

Methods belonging to the second subcategory measure changes in the pillow pressure [65, 76] or changes in the pressure of the mattress [14, 70]. In [65], two sensors measure the changes in the pressure of an air pillow placed under patient's occiput. Independent Component analysis was then used to extract three sources of information: heartbeat, respiration and noise from the two observation vectors (two pressure sensors). Since extraction of three sources from two observation is an under-constrained problem, a band-pass filter was used to segment heartbeat signals from respiration.

In [70], an air sealed cushion is placed under the mattress. Changes in the cushion air pressure is measured by a pressure sensor that has a flat frequency response between 0.1 and 5 KHz. The sensitivity of the sensor is 56 $\frac{mV}{Pa}$. This system was able to detect respiration, posture, movements, apnea and snoring. A relatively high signal to noise ratio was achieved. That is due to the fact that their sensor had a wide dynamic range and they used expensive high quality digital signal processors.

Finally the third class in sensor classification are the vision based sensors. In this class, CCD cameras are used as image sensors. Respiration is related to the optical

flow in the image sequence. In [41], an image processing board (IP) with 256 CPUs was used to compute the optical flow in the image sequence of a subject's body captured by a CCD camera. They have shown that periodic fluctuations in the optical flow represent the respiration. As opposed to respiration, posture changes cause large peaks in the optical flow.

A spatio-temporal local optimization method was used in [42] in order to compute the optical flow in the image sequence. The same characteristics as in [41] was used to determine respiration and posture changes.

The non-retraining methods described above use expensive sensors or combinations of multi-modal sensors to detect respiration, apnea and movements. In some cases, they are capable of detecting respiration only. We propose a method for detecting respiration, apnea and movements during sleep using only inexpensive pressure sensors. The approach to the intelligent bed sensor is detailed in the next chapter. Similar to vision based approach our proposed approach uses computer vision techniques. However, we process pressure information using computer vision algorithms, while studies such as [41, 42] process visual information.

Chapter 3

The Intelligent Bed Sensor

The Intelligent Bed Sensor consists of two design layers: Physical and Algorithmic. It is referred to as intelligent according to this structure. Layers of the Intelligent Bed Sensor will be described in this chapter. Section 3.1 describes the physical layer of the system. The rest of the sections in this chapter discuss the algorithmic layer of the Intelligent Bed Sensor.

3.1 Description of the sensor

The Intelligent bed sensor (IBS) is a system that embeds pressure sensors in the bed sheet to be placed on the mattress. Therefore, it does not require any direct contact with the subject. This system relies solely on pressure information from the sensors and there are no other measurements involved in the process. The IBS is intended for nocturnal monitoring in order to evaluate the quality of sleep. For this purpose, the IBS detects apnea events and movements as well as normal respiration periods. Sleep related information is logged by the system for later review.

The IBS employs a modified bed occupancy sensor (BOS) by Tactex Control to measure and record information about the pressure exerted on the bed by the subjects' body. The bed sensor consists of 144 optical pressure sensors forming 6 adjacent

sheets of sensors. Pressure sensors are placed on a regular 3x8 inches grid in each sheet. Each sensor indicates a value that corresponds to the amount of pressure being exerted on it. Since these sensors do not measure the absolute pressure, the output value does not have a unit. Optical pressure sensors used in this study are based on multiple reflections formed in the Fabry-Perot cavity between two mirrors. The characteristics of the Fabry-Perot cavity change as the result of the pressure exerted on the sensor that causes a diaphragm to bend, leading to changes in the reflected light intensity. Optical pressure sensors are low cost and could be implemented on a large scale using semiconductor growing and micro-machining methods. A sensor diameter of as small as 100 um is achievable using a single multi-mode optical fiber [64]. Measured pressure is digitized and transmitted to a computer via the data acquisition (DAc) box that samples each sensor at 5.3 Hz. Digitized pressure data is transmitted to the computer station via the serial port. Data acquisition and logging software has also been provided by the sensor manufacturer and is used to record the pressure data on computer storage media, such as a hard disk.

A first version of the Intelligent Bed Sensors is described in [11]. This version uses a smaller bed sensor and a different signal processing approach. Pressure values from 24 pressure sensors have been used to create a sequence of pressure maps. The video sequence is then processed using the concept of inter-frame similarity matrix (IFSM). Periodicity is extracted from edge signals in the IFSM filtered using a Wiener filter to enhance detection of local extrema. This approach introduces a large amount of redundant information during pressure map generation. There are 24 pressure signals available as sources of information that are interpolated into pressure maps. This process generates redundant information and subsequently increases processing load. The approach in [11] has not been tested on long video sequences. The approach investigated in the current study aims to process the pressure data directly using the

IFSM.

3.1.1 Summary of the approach

Once pressure data for a study session is acquired, it is first pre-processed to remove noise. Afterwards, movement events are detected from the data using a statistical method. The Filtered data is used to create a video sequence of inter-frame similarity matrices of a window that is slid over the data. The result is referred to as a sliding inter-frame similarity matrix video (SIFSM). This video is segmented using a watershed transformation method. Regions of interest are extracted from the segmented video to avoid unnecessary processing of the whole frame. A region descriptor, Compactness (also known as circularity), is used as the criterion for classifying individual regions as normal respiration or artifacts. The next step of the algorithm further classifies artifact regions into apnea or movement classes and creates a color coded video file containing these regions. Eventually, the study log file is created from the color coded video.

The rest of this chapter will discuss the steps mentioned above in more details.

3.2 Data Acquisition

Data acquisition and logging software was provided by the sensor manufacturer and was used to record the pressure data on computer storage media. The pressure log files are comma separated value (.CSV) files that are accessible using Microsoft Excel or Open Office Calc. The software splits the log file every two minutes of acquisition. Each log file has a unique file name that contains the date and time of the acquisition. We have developed a routine that reads .CSV files in MATLAB, converts them into MATLAB matrix format and saves them for later reference.

Data: Folder containing a set of .CSV files
Result: Single data matrix ready for processing
while *end of last file has not reached* **do**
  read a new line from currently open .CVS file;
  separate values and create a vector;
  append the vector to data matrix;
  if *last line of the file* **then**
    close current file;
    open the next .CSV file;
  end
end

Algorithm 1: Converting multiple .CSV files to a single data matrix

Algorithm 1 concatenates all log files created by Tactex Co. software in the form of a matrix. As a result, the pressure observation is presentable in the form of an ordered set:

$$\bar{X_k} = \langle x_1, x_2, ..., x_{144} \rangle \,, \tag{3.1}$$

where sub-observations x_i are kth sampled pressure values. The length of each vector depends on the length of the observation, in other words, acquisition duration.
The system setup for data acquisition is shown in figure 3.1. The Video camera and microphone recorded additional information to be used for evaluating the IBS and are not part of the system.

3.3 Preprocessing

The main challenge for processing pressure data is the presence of noise from two sources: sensors' innate noise and movement artifacts. Each type of noise is detailed below.
The sensors' innate noise can be characterized as amplitude modulation of a very low frequency and a high frequency component. The low frequency component becomes

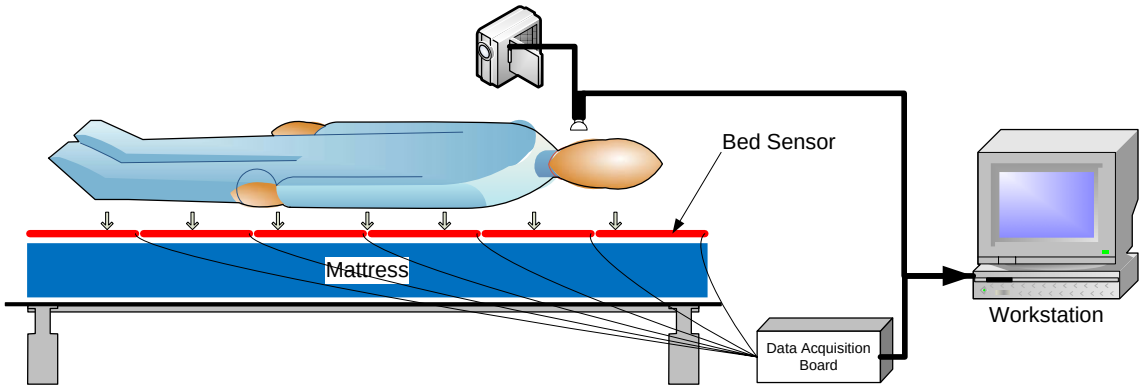

Figure 3.1: Diagram of the Data Acquisition system. The video camera and microphone were used for collecting ground truth data

dominant in sensors that are under pressure, i.e. it is negligible in sensors recording zero. The effect of this component of noise is a base line drift in recorded values over time.

The high frequency component of the noise is due to the uncertainty involved in quantizing the pressure in the electronic circuit. This introduces rapid fluctuations in digital values. This rapid fluctuation is the main contribution to the high frequency component of the noise. Therefore it is assumed to be conditionally independent and Gaussian with zero mean. In other words:

$$p = \frac{1}{\sqrt{2\pi}\sigma} exp(\frac{-x_i^2}{2\sigma^2}). \tag{3.2}$$

Where p is the probability density function and σ^2 is the variance of the noise.

Also, the movement of the patient is a source of noise in the data, since it creates large spikes in the readings of involved sensors. Most movement induced noises are spikes. They also contribute to the high frequency portion of noise and thus are treated in the same manner. Since movement is one of the parameters that the IBS is intended to monitor, a robust approach is needed for segmentation of movement events from pressure values in the presence of noises such as those described above.

In order to prepare the data for further processing, a high pass filter with character-

istics shown in figure 3.2 was used. This preprocessing step eliminates the DC value of the pressure as well as the base line drift. It will therefore enhance the system's overall dynamic range as shown in figure 3.4. Nevertheless, the high frequency components of the noise are not affected by this filter. They are eliminated using image enhancement techniques after converting the data into video sequences as described in section 3.6.

3.3.1 Movement Detection from pressure data

Signal characteristics that are caused by the subject's movements are used to detect movements during sleep. Jones et al. [31] have proposed a method for detecting movement from pressure data acquired by sensor arrays. We used the same adaptive method to determine average and standard deviation of the pressure data over a sliding window of samples. Standard deviation and average value of the samples from all sensors are calculated as the window size increases. When the window size reaches 100 samples the window begins to slide over the data. At every step the next value of the channels are compared to Upper and Lower Thresholds defined by equations 3.5 and 3.6.

$$p(LT < x_i < UT) = 0.99, \tag{3.3}$$

$$\int_{LT}^{UT} \frac{1}{\sqrt{2\pi}\sigma_i} exp(\frac{-x_i^2}{2\sigma_i^2}) = 0.99, \tag{3.4}$$

where p is the probability that sub-observation x_i not being associated with a movement. The two thresholds, UT and LT will be derived as:

$$UT = \mu_i + 3\sigma_i, \tag{3.5}$$

$$LT = \mu_i - 3\sigma_i. \tag{3.6}$$

We aim for a certainty of 99% for detection of movement from the pressure values. In other words, the two thresholds need to be determined in such way that they could tolerate noise and extract movement from the pressure signals. If the probability distribution (density) function (PDF) of the pressure data is assumed to be the normal distribution function, thresholds of $\mu \pm 3\sigma$ will cover 99.7% of the PDF area. This means any value that falls outside this range corresponds to movement with a probability of 99.7%.

Pressure values from individual sensors are tagged as movement or non-movement using the approach described above. This information is stored in a separate file to be used later for distinguishing between apnea events and movements as described in section 3.8. Algorithm 2 shows steps for movement detection.

3.4 Inter-Frame Similarity Matrix

Respiration and breathing motion are both periodic. Thus, respiration alters pressure values recorded by each of 144 sensors periodically. Ideally, a periodic signal has a fundamental period:

$$S(t + T) = S(t), \tag{3.7}$$

where T is the fundamental period. However, in practice, signals may undergo different transformation and deformations, such as translation or additive noise being introduced. Numerous approaches have been investigated for detection of the period-

```
Data: X_k  for  all k
Result: M_k  which has the same size of X_k
for i=1:144 do
    for  all k do
        if window size <100 then
            increase the window size
        else
            slide the window
        end
        compute the sigma and μ for the new window ;
        compute the new UT and LT from equation 3.6;
        if x_i and x_{i+1} >UT or x_i and x_{i+1} <LT then
            reset the window size to 1;
            mark m_i as "1" in M_k;
        end
    end
end
```

Algorithm 2: Movement event marking in data matrix

icity and mining periods in time series data. However, periodicity mining in presence of noise is a challenging problem [19]. Elfeky et al. have proposed an approach that addresses this problem [19].

All above mentioned techniques work on time series data (1D). Although the IBS source of data appears to be in the same form, pressure sensors can not be processed individually due to changes in active sources of information. Considering 144 sources of information that become active at different times due to subjects' movement on the bed, if treated as time series data, periodicity mining sounds impossible given an average signal to noise ratio (SNR) of -6 $d\beta$.

Cutler et al. have investigated a robust approach for detection and analysis of periodic motion in video sequences [17]. The concept of the inter-frame similarity matrix (IFSM) is based on measurement of similarity between frames of a video sequence. Various similarity metrics can be used to calculate the IFSM. Similarity can also be computed in pixel (spatial) or frequency domains. For periodic motion, the

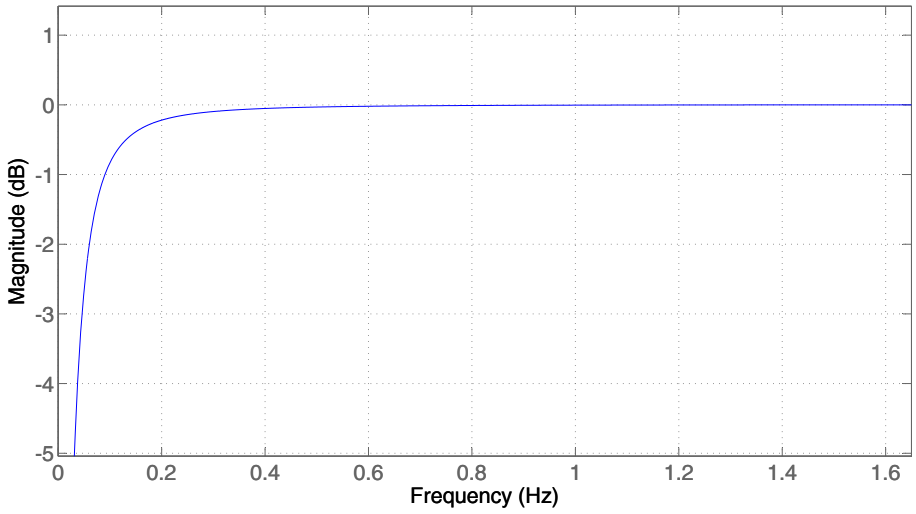

Figure 3.2: Magnitude response of the filter used for preprocessing the data. Filter Type: High Pass IIR Butterworth. Fstop: 0.02 Hz. Fpass: 0.1 Hz. Pass Band gain: 0 $d\beta$. Reject Band gain: -8 $d\beta$.

self-similarity measure is also periodic. Cutler et al. use Time-Frequency analysis for detecting and characterizing periodic motions. They also proposed 2D lattice structures inherent in similarity matrices for robustly analyzing periodicity. Their approach is successfully implemented as a real-time system that has been able to track and classify objects using periodicity. The IFSM is particularly effective for analyzing sequences containing periodic phenomena, and has been used for a variety of applications. Examples of such applications are discussed below.

In [3] inter-frame similarity is used for dropping similar frames for the purpose of video trans-coding. The authors calculate the inter-frame similarity based on the DC coefficients of the Discrete Cosine Transformation (DCT), as they represent summary information of blocks in images [10]. The frame priority assignment algorithm is based on uniform distribution of dropped frames. This minimizes jitter and maximizes the distance between two consecutive dropped frames. The Inter-frame similarity based trans-coding system was shown to be an effective approach for delivering video with

good quality to smart hand-held devices.

Another application of the inter-frame similarity matrix is in the field of medical imaging. In [46], the authors have employed the concept of IFSM in order to pick one frame per heart beat from a *pullback* video sequence. This process is referred to as *gating*. For studies of vessel morphology, plaque characterization, and other purposes that require 3-D images, the imaging sensor which is a transducer-bearing catheter can be gradually withdrawn through the vessel during recording. The recorded image sequence is called the *pullback* video sequence. A 3D volumetric model of the vessel can then be reconstructed from the pullback sequence. The motion artifacts caused by the heart beats may render these types of sequences difficult to analyze without subsequent gating.

Inter-frame similarity matrices have not only been used for detecting periodicity, but also for detection of changes and video segmentation. In [16], the concept of IFSM has been used for detection of changes in the scene(scene boundary detection). It has been shown that the IFSM outperforms histogram based techniques for detection of changes in the video sequence.

The similarity matrix translates temporal periodicity into spatial, textural periodicity. Changes in period and local aperiodic events are easily detected from the IFSM. Therefore, this concept is adequate for detecting changes in the breathing pattern, such as transitions from shallow to profound breathing (or vice versa), and apnea. The similarity matrix is particularly suitable for the temporal segmentation of periodic and symmetric motion [11]. Regular respiration is a periodic and symmetric fluctuation in the pressure values. Therefore, the similarity matrix concept was used to create the inter-frame similarity matrix (IFSM) by calculating the normalized

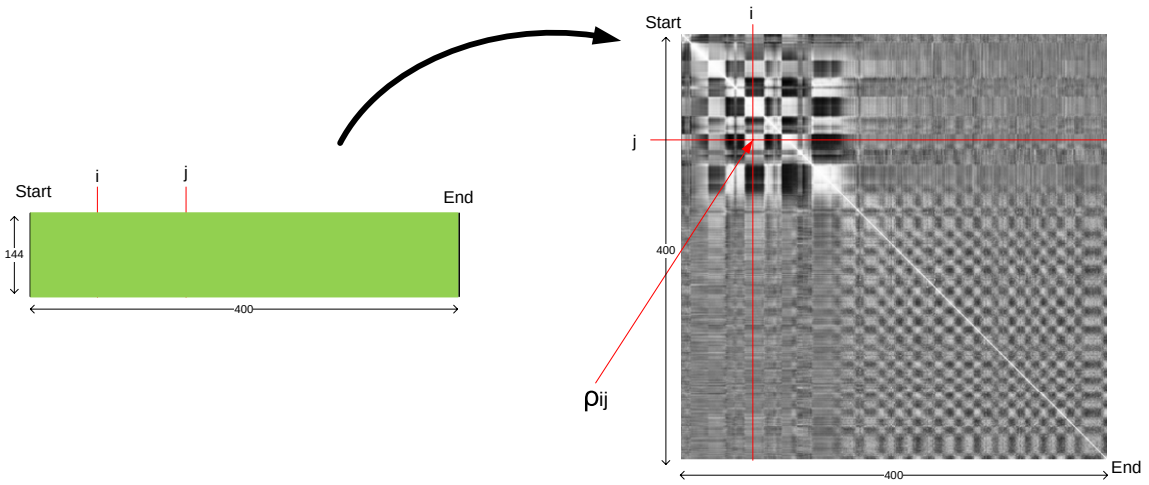

Figure 3.3: The inter-frame similarity matrix. Left: 400 samples of 144 channels in time series form. Right: IFSM computed for the data

cross-correlation of pressure value vectors using equation 3.10. Each vector consists of 144 pressure values from the sensors.

$$\forall\ i\ \in\ [acquisition\ length]\ , \qquad \mu_i = \frac{1}{144}\sum_{l=1}^{144} x_l, \tag{3.8}$$

$$\rho_{ij} = \frac{\sum (X_i - \mu_i)(X_j - \mu_j)}{\sqrt{\sum (X_i - \mu_i)^2 (X_j - \mu_j)^2}}, \tag{3.9}$$

$$IFSM = [\rho_{ij}]\ \forall\ i, j\ \leq\ N, \tag{3.10}$$

In equation 3.10, ρ_{ij} denotes the similarity between vectors (frames) X_i and X_j. μ_i and μ_j are mean values of vectors (frames) X_i and X_j respectively. ρ will always hold values in the range of $[-1, 1]$ according to the Cauchy–Schwarz inequality [1]. A similarity value of 1 corresponds to the similarity of two identical vectors, such as ρ_{ii}. A complete inter-frame similarity matrix will contain N^2 elements, where N is the number of vectors.

3.4.1 Sliding Inter-Frame Similarity Matrix

Calculating the IFSM is a computationally expensive process. On the other hand, sleep monitoring data usually consists of large numbers of vectors, which in turn

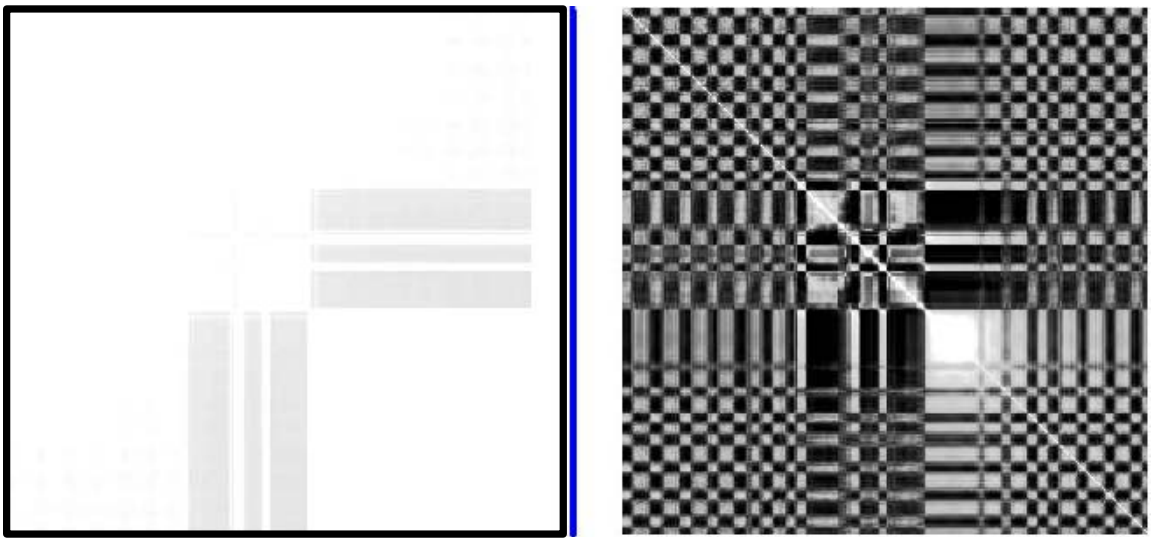

Figure 3.4: The inter-frame similarity matrix. Left: IFSM computed from unfiltered data. Right: IFSM from filtered data as described in section 3.3. The preprocessing step enhances the overall dynamic range.

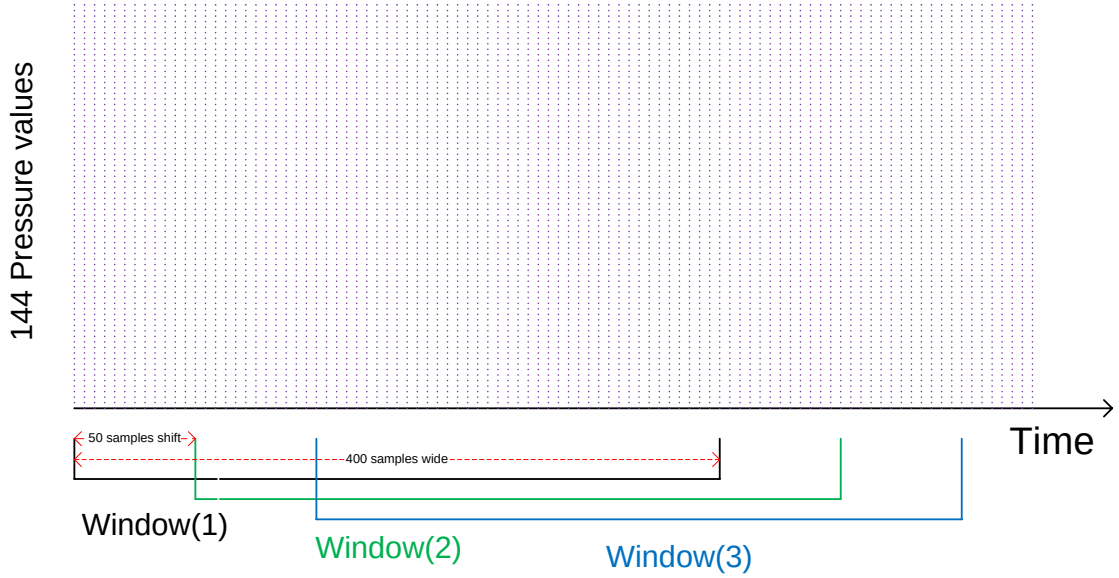

Figure 3.5: The sliding window concept. The IFSM is calculated for each window above. A sequence of IFSMs calculated for a dataset is referred to as the SIFMS video.

increases the computation cost dramatically. In order to address the computational cost problem, a sliding window of vectors was selected for creating the IFSM. This is referred to as the sliding inter-frame similarity matrix (SIFSM). The SIFSM is a video sequence of similarity matrices calculated for each selected window. The window size (number of vectors) was defined to be 400 samples, which corresponds to 75 seconds of pressure data sampled at 5.3Hz. At each iteration, the window is shifted 50 samples (9.5 seconds) and the SIFSM is calculated. This means that each frame in the SIFSM video has 9.5 seconds of new information appended to it and the oldest 9.5 seconds are shifted out of the frame. Since the main diagonal consists entirely of auto-correlation values, it represents a white line for any selected window. The sliding window for creating the SIFSM is demonstrated in figure 3.5. The SIFSM video was processed as described in the following sections. Algorithm 3 demonstrates the steps in creating the SIFSM video sequence.

Data: $X_k \quad for \quad all \; k < K$
Result: SIFSM Video Sequence
open new video file: SIFSM;
for *k=1, increments of 50, until* $K - 400$ **do**
    Compute current frame: IFSM, using equation 3.10 ;
    Write IFSM to the video file;
end
close SIFSM video file;

Algorithm 3: Creating the SIFSM video

3.5 Time Series versus the IFSM: A Discussion

As discussed in section 3.4, characteristics of the data channels change over time according to the changes in posture or movements on the bed. Figure 3.6 shows 15 channels of a pilot study plotted against sample numbers. In this figure, samples that are affected by subject's movements are highlighted in red. Note that, for instance, the channel marked as 'data 13' (third plot from the top) in the legend, becomes

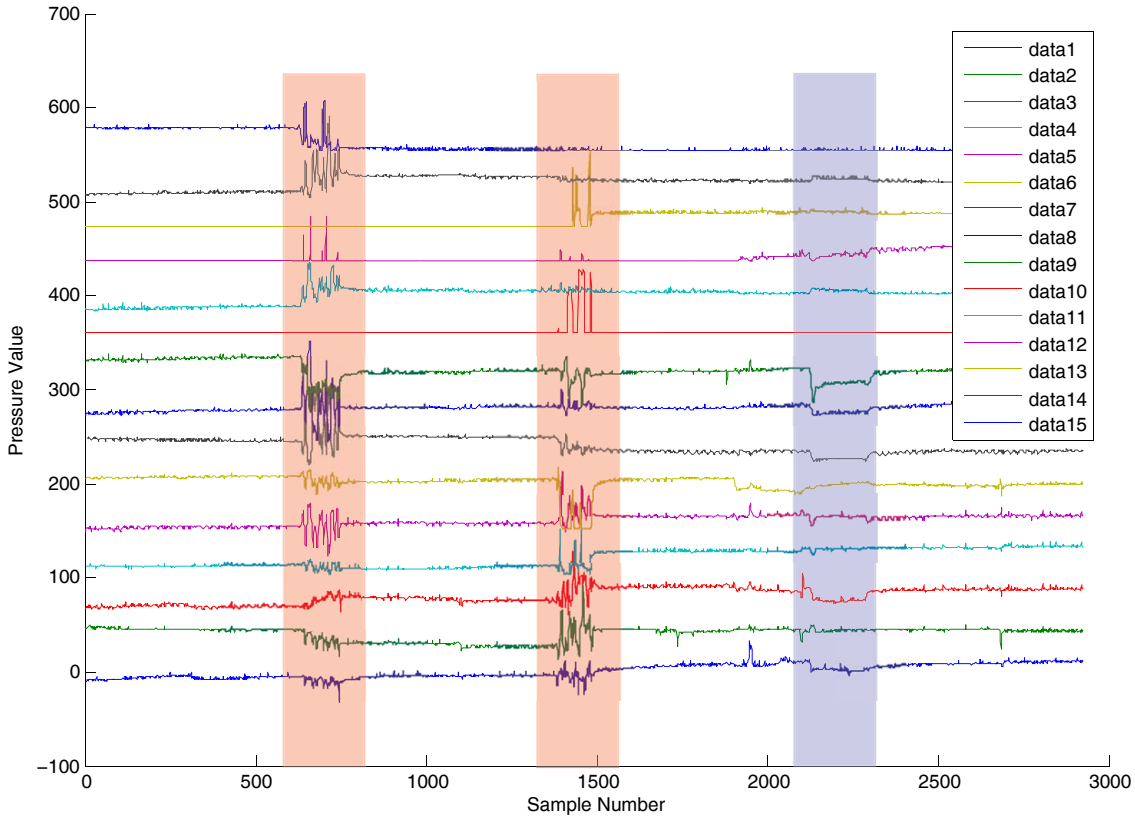

Figure 3.6: 15 pressure channels plotted against sample number in a 9 minutes long pilot acquisition

active only after the second movement period. In another example, channels marked as 'data 10 and 12' (4th and 6th) are only active during the movements and are recording zero almost all other times. In almost all the channels displayed in figure 3.6, there is a noticeable change in the mean value of the channel that is caused by the movements.

The area highlighted in blue corresponds to an apnea event. The effect of noises can be clearly seen in this region where very little or no pressure changes are occurring. The change in the mean value of the channels is still present during the simulated apnea event.

Poor Signal to Noise Ratio (SNR) and sudden changes in characteristics of pressure channels, make detection of periodicity a quite challenging task. Therefore, the

pressure data is considered as a matrix instead of a set of time series data to allow application of the IFSM. Using the IFSM, periodicity can be detected robustly, even in the presence of a large amount of noise. Periodicity in time is translated to periodic texture in pixel domain. Figure 3.7 shows the similarity matrices corresponding to highlighted regions in figure 3.6. In this figure, the top left figure represents the IFSM computed for an empty bed. This figure clearly shows the amount of noise in the system and its effect on the pressure data. In an ideal system, where there are no noises interfering with the signal, the IFSM will be a matrix with all elements equal to 1. That is due to the fact that in equation 3.10,

$$\mu_i = X_i \quad and \quad \mu_j = X_j, \tag{3.11}$$

$$\sqrt{\sum (X_i - \mu_i)^2 (X_j - \mu_j)^2} = \sum (X_i - \mu_i)(X_j - \mu_j), \tag{3.12}$$

$$\rho_{ij} = \frac{\sum (X_i - \mu_i)(X_j - \mu_j)}{\sum (X_i - \mu_i)(X_j - \mu_j)}, \tag{3.13}$$

$$\forall\ i, j\ \in\ [N] \qquad \rho_{ij} = 1. \tag{3.14}$$

The top right sub-figure highlights the apnea event in figure 3.6. It could be seen that there are a few slight movements occuring during the apnea. This is represented by the irregular noisy checkerboard patterns in the top left and bottom right corners of the highlighted area. Note that these slight movements are almost dissolved in the noisy pattern of the apnea. That is due to the small changes in pressure values induced by these movements.

In the two bottom sub-figures of figure 3.7, movements induce larger changes in pressure values. Therefore, these movements have clearer irregular checkerboard patterns. The transition period between the end of movements and the first cyclic respiration detected afterwards is also important. This transition period is represented by a bright region that begins at the end of each movement event and gradually fades into cyclic respiration patterns. This period is caused by sudden large change in sensor

values as a result of a sudden movement. A large sudden change in amplitude is similar to a unit step. The unit step response of the filter used in the preprocessing stage is shown in figure 3.9. As could be seen in this figure, the transition time in filter response is about 8 seconds. This 8 seconds long transition time causes the bright region after each movement event in the IFSM. After 8 seconds, cyclic respiration patterns begin to fade in as the step response decays to less than 10% of its initial value.

Considering the relatively long transition time of the filter, its effect might appear to be negative. However, this filter has improving effects through enhancing the dynamic range of the IFSM as could be seen in figure 3.4. As discussed in section 3.3, it also removes the base line drift present in figures 3.6, 3.8 and 3.10.

3.6 Watershed Segmentation

The watershed transformation is a popular image segmentation algorithm for grey-scale images. The watershed has emerged as a powerful tool of mathematical morphology for image segmentation. Several very efficient algorithms have been devised for the determination of watersheds. However, the application of watershed algorithms to an image often results in over-segmentation into a large number of small, shallow watersheds, instead of a few deep ones which were intended [8]. The watershed transform generates a matrix of points of the same size as the original image, where each point has been labeled using its steepest descending path as belonging to a unique catchment basin [47]. In watershed segmentation, the image is considered as a 3D topographic map.

The three dimensions of the topographic map in this study are similarity (gray level) and spatial coordinates. Each point in this map belongs to one of the categories below:

- regional minimum
- points at which a drop of water will certainly fall into a single minimum
- points at which a drop of water is likely to fall into more than one minimum

All points that belong to the third category are referred to as division lines or watershed lines. Points in the second category form the catchment basins or watersheds. From a topographic point of view, the watershed transform represents the division of the surface into its water catchment basins.

The goal is that each catchment basin matches an object in the image. Nevertheless, the result of the watershed transform is not satisfactory, due to the fact that thousands of catchment basins arise where only a few were expected [7]. In the topographic analogy, this is similar to detecting every small pothole on the roads of a country while trying to segment the map into provinces or territories using their lakes and rivers. This problem is called over-segmentation and is mainly due to noise in the image. The best solution is to merge the catchment basins after the watershed transform [47]. One approach to watershed merging is presented in [8]. Generally, it addresses the problem of finding the closest image that has a simpler watershed structure than the original segmented one. The basic idea is to replicate merging of real watersheds as happens when rain falls over a landscape: smaller watersheds progressively fill until they overflow. The water then flows to a nearby, larger or deeper watershed, in which the overflown watersheds are merged. The effectiveness of this approach is demonstrated for several biomedical applications [8].

Watershed segmentation offers more stable segmentation results compared to edge detection algorithms: continuous boundaries [24]. Every frame in the SIFSM video needs to be segmented into regions, and it is crucial that these regions are separated by continuous boundaries. Therefore, the watershed segmentation technique is an adequate method for segmentation of the IFSM.

There were two components of noise added to pressure data. The low frequency component was removed by the preprocessing step described in section 3.3. However the high frequency component of the noise, which is still present in the SIFSM, leads to over-segmentation by watershed transformation. In order to avoid over-segmentation, each SIFSM frame is filtered using a 5x5 averaging filter prior to watershed segmentation. The result of watershed segmentation of a frame of the SIFSM video is shown in figure 3.12.

3.7 Extracting Regions of Interest

The IFSM has a set of characteristics that makes it a robust tool for detecting periodic phenomena:

(A) Every cyclic and symmetric activity has a corresponding pattern aligned on the main diagonal of the inter-frame similarity matrix. Therefore, the upper-left and lower-right corners of the bounding box enclosing the pattern correspond to the first and last vectors of the activity, respectively (see figure 3.13, left). This observation is fundamental for the accurate temporal detection of breath cycles in the SIFSM video [1].

(B) Each complete breath cycle corresponds to a combination of two bright and two dark regions (see figure 3.13, left) in the IFSM. A complete cycle is represented by a diamond shaped boundary containing four catchment basins in the watershed segmented image (see figure 3.13, right). Changes in breath depth result in bounding boxes of different size. Trivially, profound breathing results in larger bounding boxes compared to shallow breathing. Figure 3.13 shows the inter-frame similarity matrix for a sequence with two different breathing patterns: profound and shallow.

Since every respiration cycle has a corresponding checkerboard pattern on the main diagonal, the region of interest can easily be extracted from the matrix to reduce computational costs. For this purpose, all the regions that are aligned on the main diagonal are kept and the rest of the regions are discarded. Also, in order to avoid the irregular shapes close to image boundaries, regions adjacent to image boundaries are removed as well. Removing boundary regions only causes a loss of information in the first and last frames of the SIFSM video. This is due to the sliding window nature of the video. For all frames other than the first or last, boundary regions will also be contained in either previous or future frames, and will not be located on the boundary of the frames. Figure 3.13, right, shows the result of this process.

3.8 Region descriptors

Classification of regions in images is one of the most important and active topics in computer vision and image processing, with many applications in image retrieval, computer aided diagnostics, etc. Recently, the local feature based method has become popular in image categorization due to its flexibility, simplicity, and good performance [34]. Small regions are segmented in an image and descriptors are used to describe them in a more compact way. Using different descriptors leads to extracting different information for image representation. A number of algorithms for describing image regions have been reported in literature. The most simple way is using the color or intensity value in the region directly. Examples of region descriptors are: compactness, rectangularity, elongatedness, eccentricity, moments, etc. [30, 35].

After extracting the regions of interest in the SIFSM video, each frame needs to be processed in order to extract respiration cycles, apnea events, posture changes and movements. Cyclic and symmetric respiration is represented by checkerboard

patterns in the IFSM and consequently diamond shaped regions after watershed transformation. Any interference with the normal respiration cycle yields changes in patterns present in the IFSM and the shape of regions in the watershed segmented image. Therefore, a robust descriptor is needed to distinguish between normal respiration patterns and artifacts in the video sequence. The region descriptor needs to be independent of the size of the region. This is crucial to accommodate classification of respiration cycles of various lengths.

3.8.1 Compactness

One of the descriptors which is independent of the size of the object, is the compactness or circularity. It is calculated as:

$$C = \frac{P^2}{A} \tag{3.15}$$

where P is the perimeter of the region and A is the area or the number of pixels in the region [30]. Compactness has an absolute minimum of 4π for a perfect circle region. The compactness of a square is always 16 and that of an equilateral triangle is $12\sqrt{3}$. Compactness of elongated shapes are usually higher than the above values. In this study compactness has been chosen as the classification criterion to classify individual regions in the segmented SIFSM. Each region is assigned to respiration class if its compactness is less than that of a square (i.e. less than 16). Regions with higher compactness values are assigned to the artifact class and are further classified into two categories: Apnea and Movement, by using the information about detected movements as described in section 3.3.1. Classes are color-coded and result in another video sequence. The output video sequence has the same length as the original SIFSM video and contains only the regions of interest in each frame color coded representing the class to which they belong. Figure 3.14 shows a frame of the

output video sequence.

3.9 Sleep Study Log

The final step in processing sleep information is creating the study log file. This is the output of the IBS that can be viewed without special tools. The log file contains information about apnea movement events. It can be viewed using ordinary text viewers such as Wordpad or Notepad. Individual respiration cycles, apnea events and movements are also logged with their start and end times. There are two types of log created by the IBS as output. The following will cover the two types of log and the methodology for creating them.

3.9.1 Detailed Log

This is the fist output of the IBS. Detailed log contains information about all the events during the acquisition. Detailed log is created directly from the color coded video by grouping every 4 neighbor regions in the video. Region grouping is based on the fact that each complete cycle of respiration consists of 4, ideally square, regions (refer to section 3.7). In case one or more of the adjacent regions have a different color from the rest, the dominant color is considered the color for the whole group. The dominant color is decided blue if two or more of the regions are colored blue; it will be red if one or more of the regions are red and green otherwise. There is a priority of colors: red has the highest, blue is second and green is last. That means if one or more regions in the group are red, the group will be considered red, regardless of the rest of the region. If two or more regions are blue and there is no red in the group that group is considered blue. Only if at the most one region is blue and there is no red in the group, that group is considered green. The system marks the beginning and the end of each respiration cycle by finding the bounding box containing a group

of four adjacent regions. Since the regions are rarely perfect squares, the bounding boxes are mostly larger by the amount of a few pixels. Therefore, the intersection of the bounding box and main diagonal of the image returns a subpixel value as could be seen in log snapshots listed in tables 3.1 and 3.2. This is due to the fact that the main diagonal of a 400 by 400 sqare images is a line with a 45° angel and $\sqrt{2(400)^2} = 565.6854$ pixels length. Depending on the dominant color of each group, they are logged in respiration, apnea or movement columns of the log. The final log is in the form of comma separated (.CSV) spread sheet that can be viewed in Excel, Open Office Calc or any text editor. A snapshot of a detailed log can be seen in table 3.1. Algorithm 4 is used for creating the detailed log. In this algorithm t indicates the time and the equation used for calculating it is based on the fact that between every two consecutive frames in the SIFSM video, there is a shift of 50 samples (pixels). Therefore, the following equation could be used in order to convert between time and pixel domains,

$$t \ \ (sec) = \frac{CurrentPixelNumber + 50(CurrentFrameNumber - 1)}{Fs \ \ (Hz)}. \qquad (3.16)$$

3.9.2 Final Log

The detailed log lists a number of events that are much more numerous than the actual number of events. This is due to the fact that an event in the real world is represented by numerous regions in the color coded video and detailed log reports groups of four adjacent regions. Therefore, it is necessary to process the detailed log to establish a relationship between actual events in the real world and logged temporal boundaries. This step is done by processing the detailed log and regrouping a number of logged events as a single event. As could be seen in table 3.1, a series of movement events was started at 12:51 (min:sec) onset the beginning of the acquisition followed by a recorded apnea event. This sequence of events in the detailed

log represents one actual event in the real world. By referring to the ground truth video it could be seen that there is a posture change event at that moment. This event has been marked correctly a single movement as listed in table 4.6 row number 22 (subject "NY"). The following will elaborate on the algorithm that groups the sequences, such as one described above, to a single event.

Sleep Log Post-Processing

The log post-processing algorithm analyzes a window of events in the detailed log. Algorithm 5 describes the steps involved in sleep log post-processing. It is assumed in this algorithm that a stable respiration pattern consists of at least four consecutive respiration cycles, shallow and/or profound. This algorithm writes the respiration cycles logged in the Detailed Log file into the Final log file without any changes. Apnea and movement events that are in the form of sequences of events in the Detailed Log file are grouped into a single event. The type of the event is determined according to the dominant event in the sequence. The algorithm starts by reading a line from the Detailed Log file, if the line indicates a respiration, it will be written into the Final Log unchanged. If the line indicates an event (apnea or movement), it is kept in the memory as the first entry to a window. The algorithm then reads a new line from the Detailed Log and keeps appending newly read lines to the window mentioned above. The window grows as long as 4 consecutive respiration cycles have not been read. Once complete, the window is considered one event. The type of the event is determined by the number of occurrences of each event type. Once the type of the window is determined, the beginning of the window will be written as the beginning of the event and the end of last event in the window is written as the end of the event in the Final log file followed by the 4 respiration cycles. Afterwards, the window is reset and the algorithm starts over again on the next line of the Detailed Log file.

The Final Log corresponding to the snapshot in table 3.1 is listed in table 3.2.

Data: Color-coded video
Result: Sleep Study Log File
Initialization: Fs = 5.3 Hz;
open color coded video;
open new study log;
while *Last video frame not reached* **do**
  find the beginning and the end of the region;
  calculate the corresponding time markers:
  $t\ \ (sec) = \frac{CurrentPixelNumber + 50(CurrentFrameNumber - 1)}{Fs\ \ (Hz)}$;
  Check the RGB channels of the current region;
  if *Region RGB value indicates Movement* **then**
    Log "Movement" between current time markers;
  end
  if *Region RGB value indicates Apnea* **then**
    Log "Apnea" between current time markers;
  end
  if *"Green"* **then**
    Log "Respiration Cycle" between current time markers;
  end
end
close video;
close log file;

Algorithm 4: Creating the Detailed Sleep Study log file

Data: Detailed Sleep Log
Result: Final Sleep Log
Initialization: open Detailed Log file;
open a new Final log;
while *Last line of the Detailed Log not reached* **do**
    read current line of the Detailed Log;
    if *Shows respiration cycle* **then**
        write the respiration information in the Final Log file;
        continue to the next line of the Detailed Log;
    end
    else
        Create new window and put current line as the first entry in it;
        Read next line of the Detailed Log;
        while *4 consecutive respiration cycles have not been read* **do**
            Read a new line of the Detailed Log;
            Add the line to the end of the window;
        end
        a=number of apneas in the constructed window; r=number of respirations in the constructed window; m=number of movements in the constructed window; **if** *m=0* **then**
            Write the beginning of the window as the beginning of an apnea event in the Final Log;
            Write the end of the last Apnea event in the window as the end of the Apnea event in the Final Log;
        end
        if *a=0* **then**
            Write the beginning of the window as the beginning of a movement event in the Final Log;
            Write the end of the last movement event in the window as the end of the movement event in the Final Log;
        end
        if *a>0 and m>0* **then**
            if $m > \frac{Window\ \ size}{5}$ **then**
                Write the beginning of the window as the beginning of a movement event in the Final Log;
                Write the end of the last event in the window as the end of the movement event in the Final Log;
            end
        end
        else
            Write the beginning of the window as the beginning of an apnea event in the Final Log;
            Write the end of the last event in the window as the end of the apnea event in the Final Log;
        end
    end
end
close Detailed log file;
close Final log file;

Algorithm 5: Sleep Study log post processing.

Frame	R_S_P	R_E_P	A_S_P	A_E_P	M_S_P	M_E_P	Respiration Start	Respiration End	Apnea Start	Apnea End	Movement Start	Movement End
.	.	.	.	.	.	.	.	.	.	.	.	.
.	.	.	.	.	.	.	.	.	.	.	.	.
.	.	.	.	.	.	.	.	.	.	.	.	.
48	336.94	368.76					0:12:26	0:12:35				
49	317.84	348.25					0:12:35	0:12:43				
50	298.05	327.74					0:12:43	0:12:52				
50					327.04	368.76					0:12:51	0:13:3
51					321.38	359.56					0:13:3.7	0:13:14
53			312.89	343.3					0:13:29	0:13:38		
53	339.76	370.88					0:13:37	0:13:45				
54	320.67	342.59					0:13:45	0:13:51				
54	341.89	360.98					0:13:51	0:13:56				
54	360.98	378.66					0:13:56	0:14:1.3				
.	.	.	.	.	.	.	.	.	.	.	.	.
.	.	.	.	.	.	.	.	.	.	.	.	.
.	.	.	.	.	.	.	.	.	.	.	.	.

Table 3.1: A snapshot of a detailed log containing respiration, apnea and movement events. Frame column lists the frame number of the event, R_S_P and R_E_P indicate the start and end pixle number of the respiration cycle in the frame indicated. A_S_P and A_E_P are the beginning and end pixles for the apnea event. M_S_P and M_E_P indicated the beginning and end pixles for the movement event. The rest of the columns display corresponding time values in HH:MM:SS format. Conversion from frame-pixel to time is done using equation 3.16.

Frame	R_S_P	R_E_P	A_S_P	A_E_P	M_S_P	M_E_P	Event Type	Start Time	End Time
.	.	.	.	.	.	.	.	.	.
.	.	.	.	.	.	.	.	.	.
.	.	.	.	.	.	.	.	.	.
48	336.94	368.76					Profound	0:12:26	0:12:35
49	317.84	348.25					Profound	0:12:35	0:12:43
50	298.05	327.74					Profound	0:12:43	0:12:52
50					327.04		Movement_S	0:12:51	
53						343.3	Movement_E		0:13:38
53	339.77	370.88					Profound	0:13:37	0:13:45
54	320.67	342.59					Profound	0:13:45	0:13:51
54	341.89	360.98					Profound	0:13:51	0:13:56
54	360.98	378.66					Profound	0:13:56	0:14:1.3
55	327.04	360.98					Profound	0:14:0.84	0:14:10
.	.	.	.	.	.	.	.	.	.
.	.	.	.	.	.	.	.	.	.
.	.	.	.	.	.	.	.	.	.

Table 3.2: A snapshot of the Final log corresponding to log in table 3.1. Frame column lists the frame number of the event, R_S_P and R_E_P indicate the start and end pixle number of the respiration cycle in the frame indicated. A_S_P and A_E_P are the beginning and end pixles for the apnea event. M_S_P and M_E_P indicated the beginning and end pixles for the movement event. The 8th column lists the event type and the last two columns display corresponding time values in HH:MM:SS format. Conversion from frame-pixel to time is done using equation 3.16.

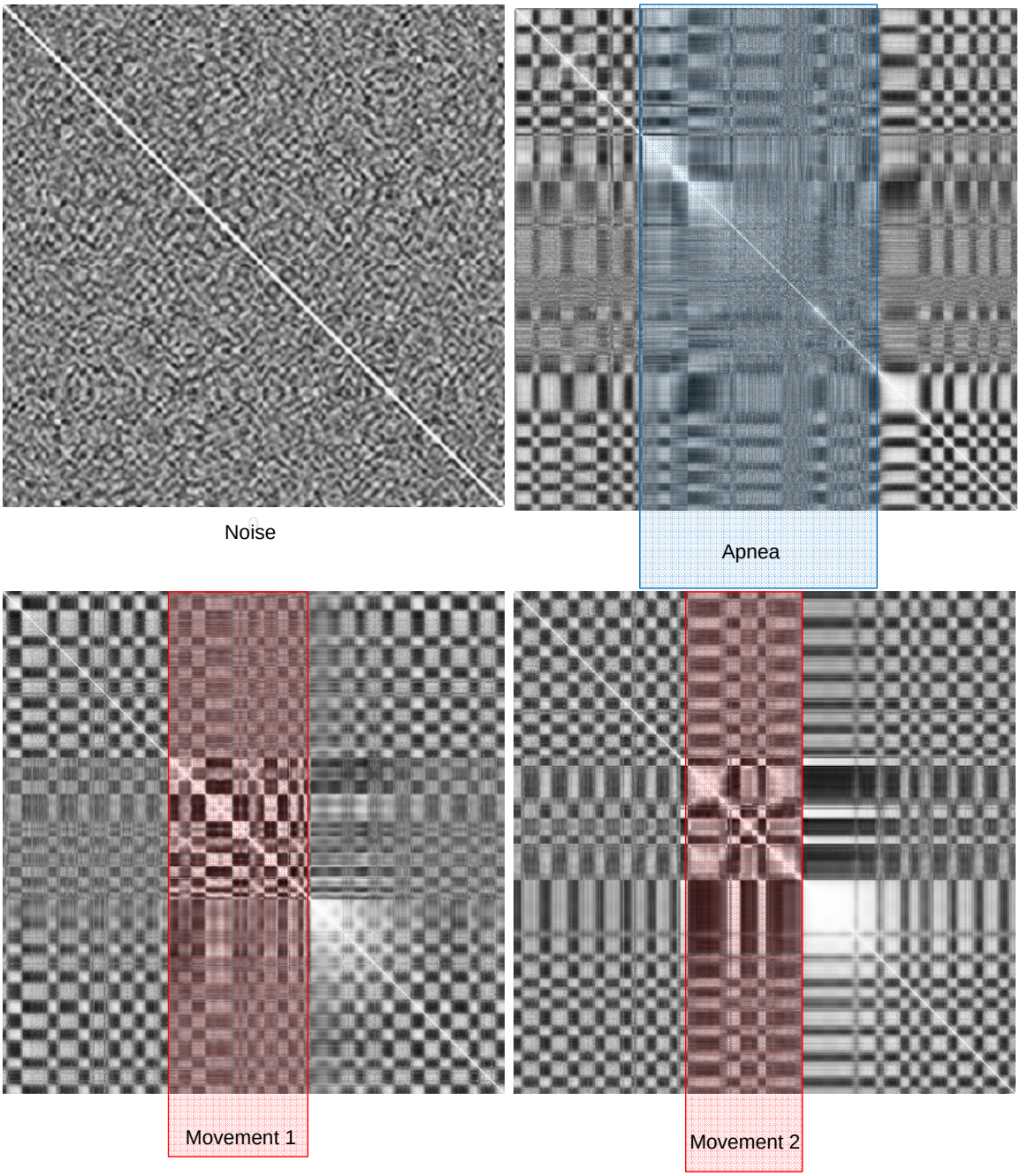

Figure 3.7: Top left: the IFSM computed for the pressure data from an empty bed. Top right: The IFSM computed for the region containing an apnea event highlighted in blue. Bottom left: Red region highlights the first movement in figure 3.6. Bottom right: Red region highlights the second movement event in figure 3.6.

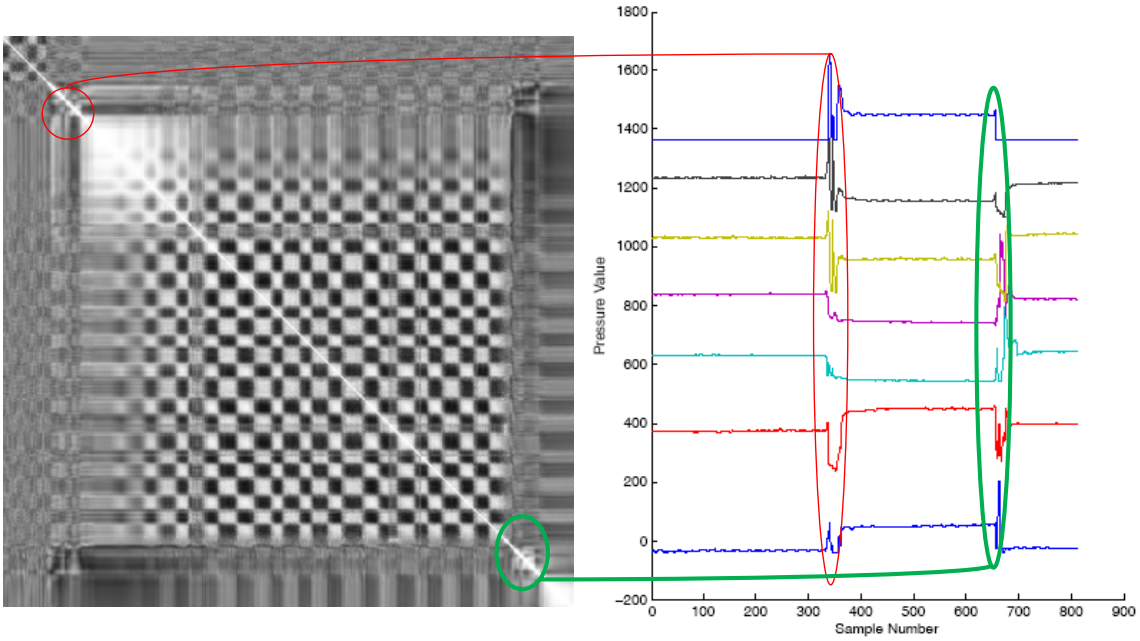

Figure 3.8: correspondence between time series data and IFSM representation. Note that, change in the posture that is present in this segment of data causes vertical shifts in the time series, but no significant change in the IFSM patterns.

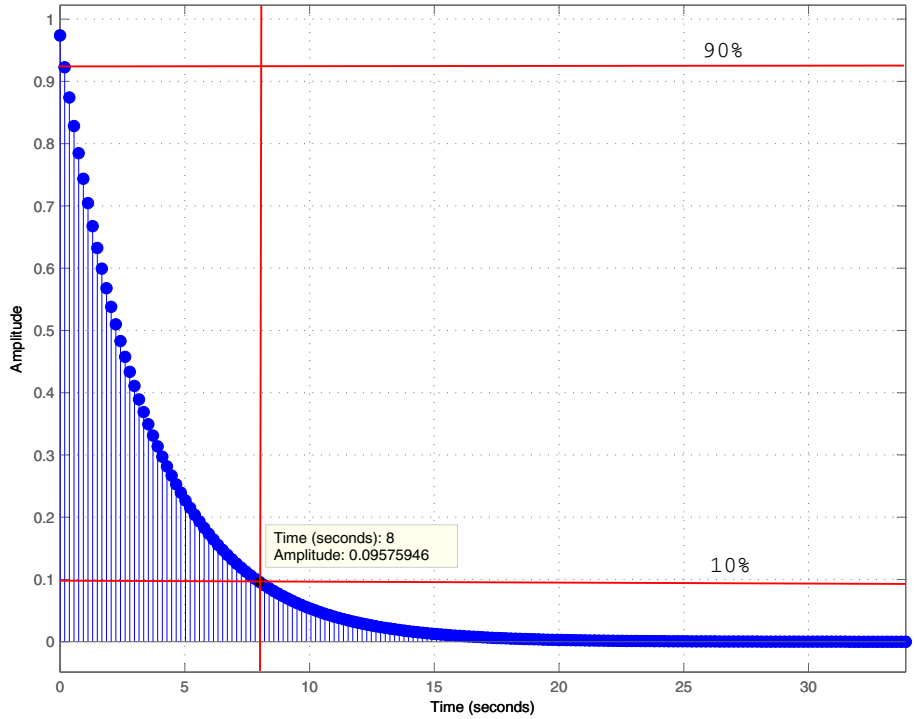

Figure 3.9: The unit step response of the filter used for preprocessing pressure data.

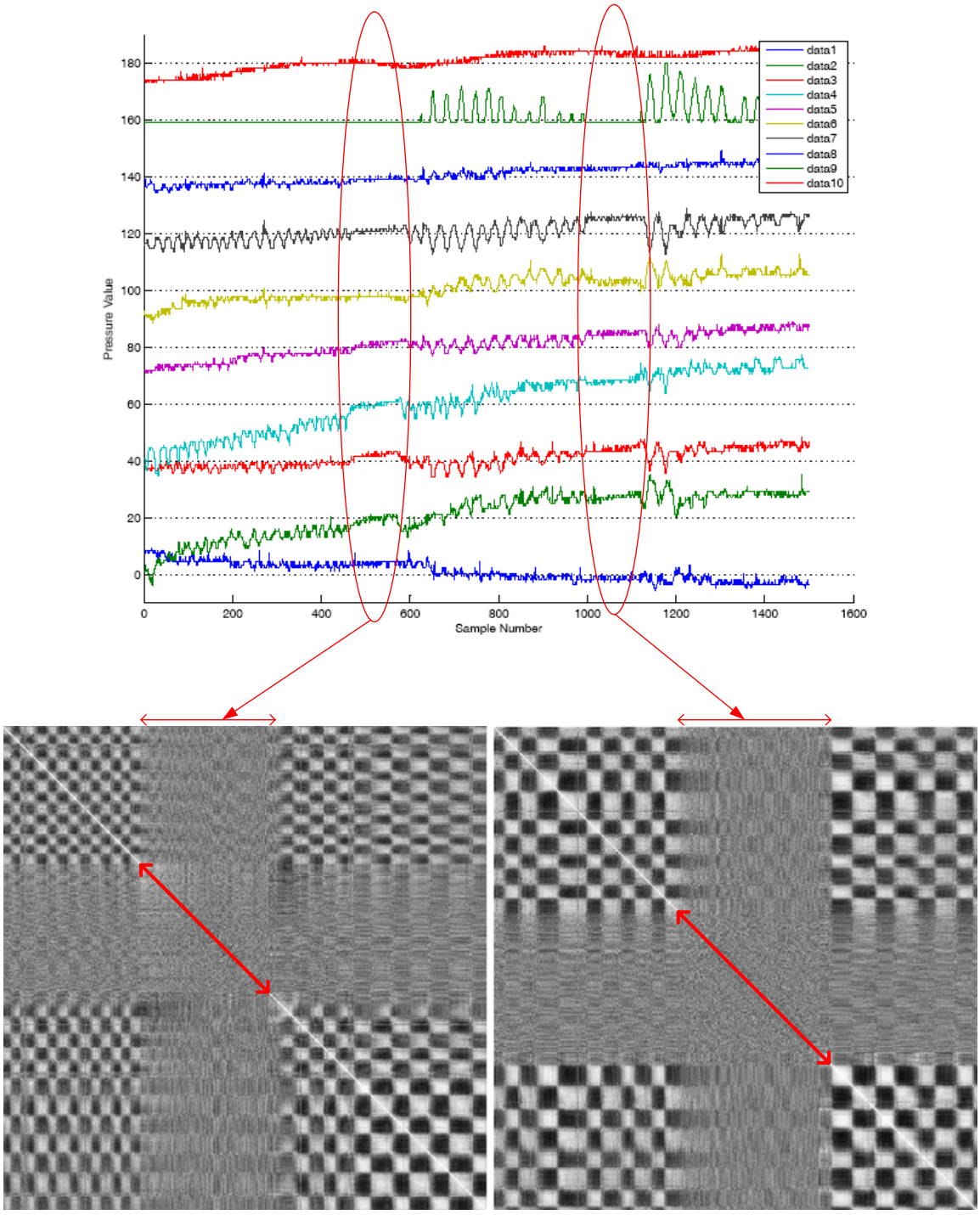

Figure 3.10: 10 pressure channels plotted against sample number. Correspondences between two apnea events are shown. The base line drift artifact, discussed in section 3.3, is also noticeable in this figure.

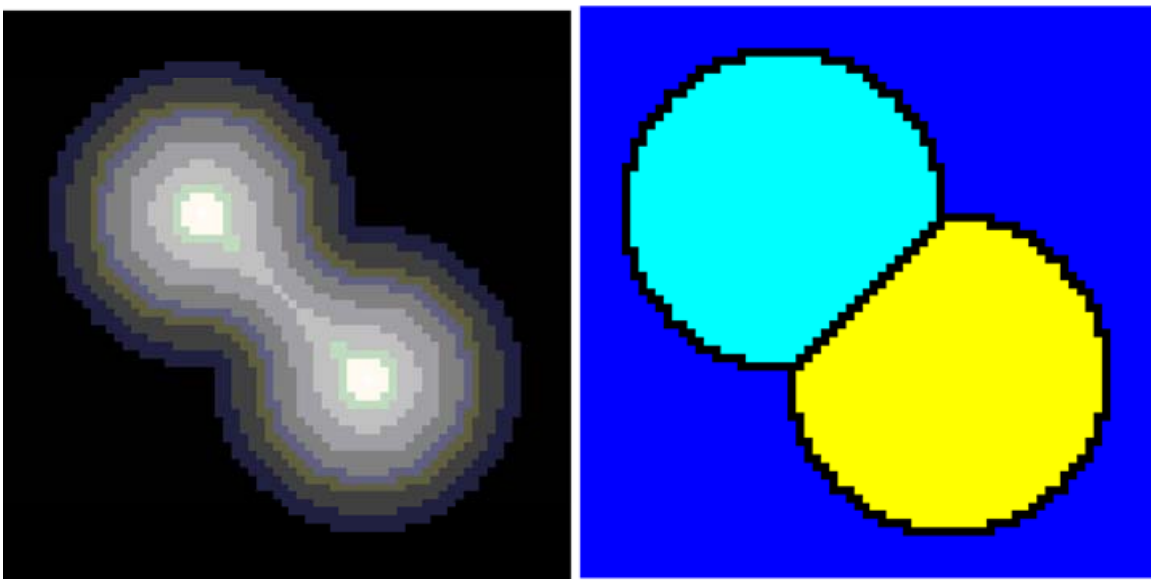

Figure 3.11: Watershed Segmentation of two overlapping regions. Left: Original image. Right: Result of Watershed segmentation.

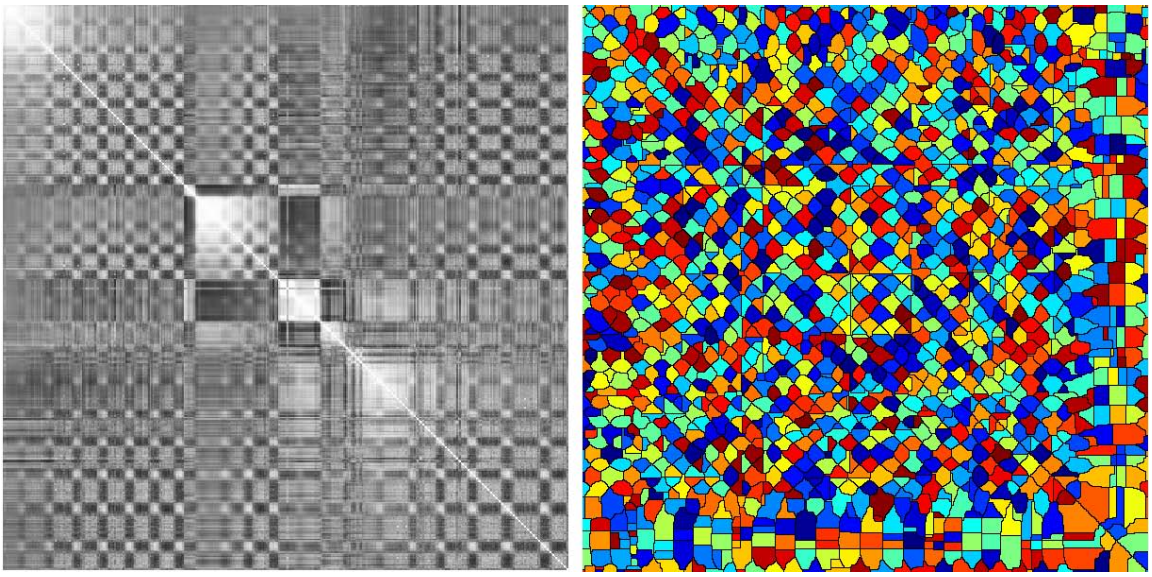

Figure 3.12: The result of the watershed segmentation (right) of a frame in SIFSM video (left). Watershed lines are shown as black boundaries between color coded catchment basins. The catchment basins, in this picture, are colored randomly for the purpose of demonstration.

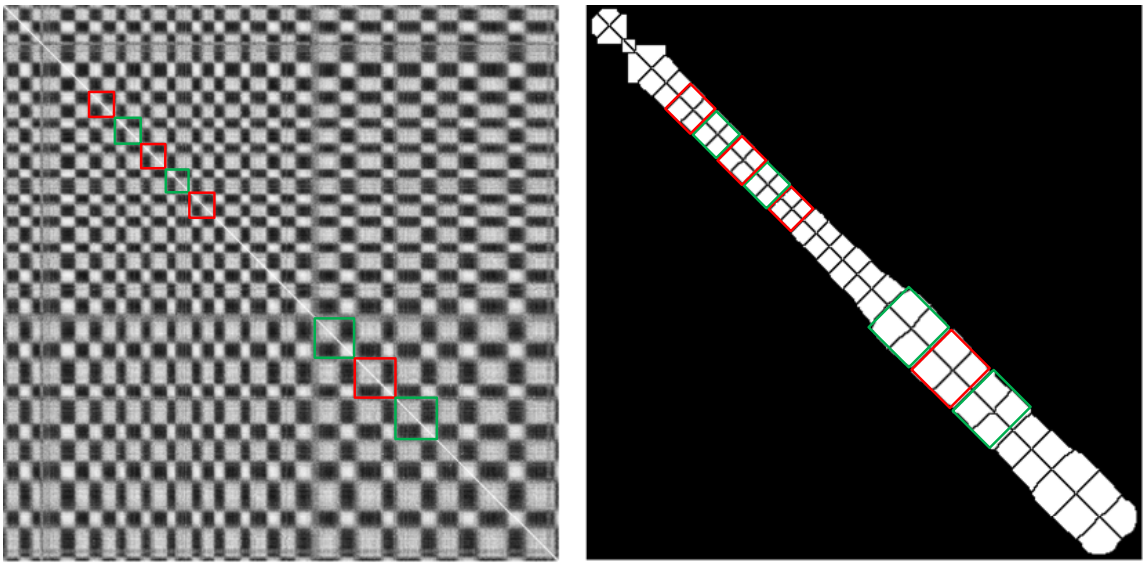

Figure 3.13: Left: A frame of the SIFSM video. Individual breath cycles are marked by bounding boxes. Note the larger bounding boxes corresponding to profound breathing in the lower right corner of the image. Right: The same frame as left after watershed segmentation and extraction of region of interest. The same breath cycles are marked by bounding boxes

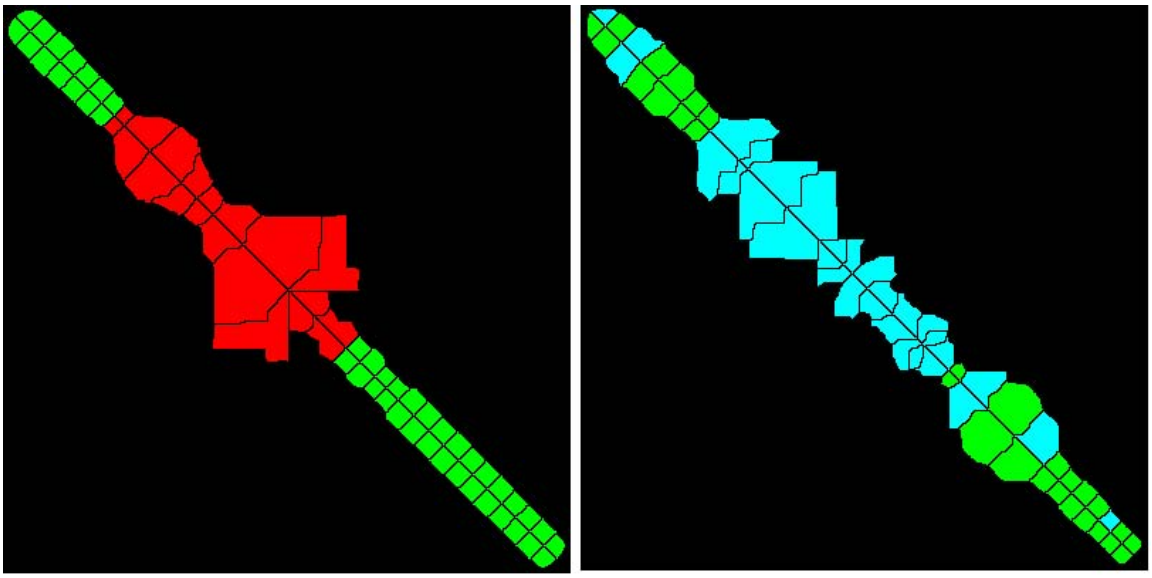

Figure 3.14: Left: A frame of the output video. Red regions are those that correspond to movements. Right: Another frame containing an apnea event represented in blue. Green regions in both images correspond to normal respiration cycles.

Chapter 4

Experimental Results

4.1 Experiment Design

In order to provide a common framework for evaluating the IBS quantitatively, the experiments were designed to be realistic and contain a statistically adequate number of events. The following will discuss the scenario developed for simulating sleep events.

4.1.1 Scenario

The scenario was designed to contain 50 events of apnea, 30 events of movements and 20 events of posture changes as basic events. In addition, shallow and profound breathing and as well as sleeping in lateral posture have also been embedded in the scenario. There was a predefined sequence of events that has been used for simulation by all volunteers. The sequence of events for each subjects is listed in table 4.1. Using the sequence listed in table 4.1 each subject simulates 2 apnea events amid shallow breathing, one apnea event between shallow and profound breathing and another two apnea events amid profound breathing. In addition, each subject will change their posture twice and breathe in lateral posture for two minutes. Following the posture

One minute of shallow breathing,
25 seconds of apnea simulation,
One minute of shallow breathing,
25 seconds of apnea simulation,
One minute of shallow breathing,
25 seconds of apnea simulation,
One minute of profound breathing,
25 seconds of apnea simulation,
One minute of profound breathing,
25 seconds of apnea simulation,
Posture change from supine to lateral,
Two minutes of shallow breathing in lateral posture,
Posture change from lateral to supine,
One minute of shallow breathing,
20 seconds of limb movement,
One minute of shallow breathing,
20 seconds of limb movement,
One minute of shallow breathing,
20 seconds of limb movement,
90 seconds of shallow breathing.

Table 4.1: Sequence of events simulated by subjects. Colors indicate the type of event. Light and dark green correspond to shallow and profound respiration respectively. Red and blue indicate movement and apnea.

changes, the subjects will three times simulate restlessness by moving their limbs for twenty seconds. The acquisition epoch ends with 90 seconds of shallow breathing. Total acquisition time is 17:20 (min:sec).

4.1.2 Presentation and Timing

The above mentioned scenario was implemented in a Power Point presentation, which provides exact timing for each event. The presentation is displayed on a monitor facing the subject on the bed. Along with the visual signals for each event, a beep-like signal is also played at the beginning and the end of each event.

4.2 Database

The database used for evaluation of the IBS was created with the aid of 10 volunteers at the University of Victoria. Using the setup described below, 7 male and 3 female young (22 to 41 years old) adult volunteers were asked to lay down on the bed with the IBS installed. Table 4.2 lists age, height and weight of each participating subject. The database gathered consists of more than 3 hours of sleep data with ground truth video and one 7-hour long acquisition performed over night. A description of the databases used in this study is following along with the methodology used for their creation.

4.2.1 Controlled Acquisitions

10 acquisitions have been conducted according to the scenario described above. During these acquisition epochs, subjects were asked to refrain from performing unnecessary movements and follow the instructions on the screen closely. The duration of the Controlled acquisitions was predefined in the scenario.

4.2.2 Uncontrolled Acquisitions

In order to confirm that the IBS is capable of processing larger datasets, an uncontrolled acquisition was performed over one night. A volunteer was asked to sleep on the bed from 11 PM until 6 AM in the next morning. This acquisition epoch is referred to by "WN" in the result tables. We consider this epoch uncontrolled, as there was no predefined scenario for acquisition.

4.2.3 Pressure Database

A pressure database is created using a modified version of the bed occupancy sensor (BOS). While the original BOS only provides the sum of the pressure values on all

Subject	Age	Height(cm)	Weight(Kg)
AM	25	194	105
ES	26	193	82
FK	41	170	66
KJ	28	179	78
MD	22	167	67
MG	28	183	82
NY	28	172	85
SM	25	160	49
SK	29	175	61
VT	36	168	72
Average	28.8	176.1	74.7
STD	5.63	11.18	15.39

Table 4.2: Subjects' information.

pressure sensors, the modified version can be used to measure pressure exerted on each one of the sensors. The modification has been made by the manufacturer: Tactex Controls Co. The BOS used for this study is made of six smaller BOSes, each one containing 24 pressure sensors and covering 36 x 11.5 inches. The complete BOS contains 144 sensors and covers the whole bed (36 x 77 inches).

Every group of 24 sensors are connected to a control board that sends optical signals to the sensors and measures the pressure. The control board also digitizes the pressure and sends it to a data acquisition board, which multiplexes the data from 6 sheets of sensors to a serial data link. The multiplexed data is sent to the computer work station for storage and analysis via the serial connection. The effective sampling frequency for each one of 144 sensors fluctuates around 5.37 HZ for acquisitions of 17 minutes long. The sweeping Sampling frequency issue is discussed in details in section 4.5.2.

Data acquisition software runs on the work station. This software, which is provided by sensor manufacturer, receives pressure data and stores them in log files in the comma separated value (.CSV) format. The .CSV files of each acquisition session were placed in separate folders and were used to create the corresponding MATLAB data structure. Two separate databases where used: pressure database and ground

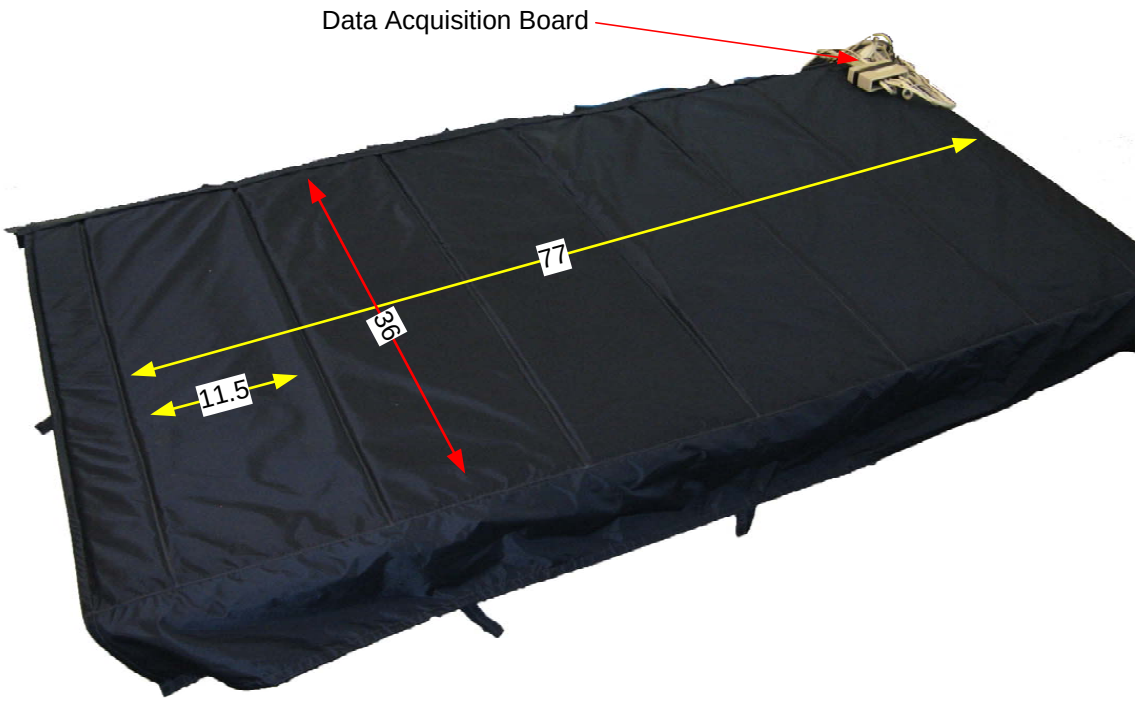

Figure 4.1: The data acquisition board and the BOS used for the Intelligent Bed Sensor. The BOS covers an area of 36 x 77 inches.

truth database. The first is the set of all data matrices built using the algorithm 1 and the latter is the set of video sequences captured by a camera.

4.2.4 Ground Truth Database

In order to have a sound reference for evaluating the intelligent bed sensor results, a ground truth database was created. Ground truth data consists of video sequences captured at 30 frames per second, covering subjects' neck to feet as could be seen in figure 4.2. In addition to visual information, respiration sounds have also been captured by a microphone hovering close to subject's mouth and nose. The microphone picks up respiration sounds that are used later to evaluate the accuracy of the system in detecting individual events during the acquisitions from pressure data.

The ground truth database is later segmented manually by a human operator. The

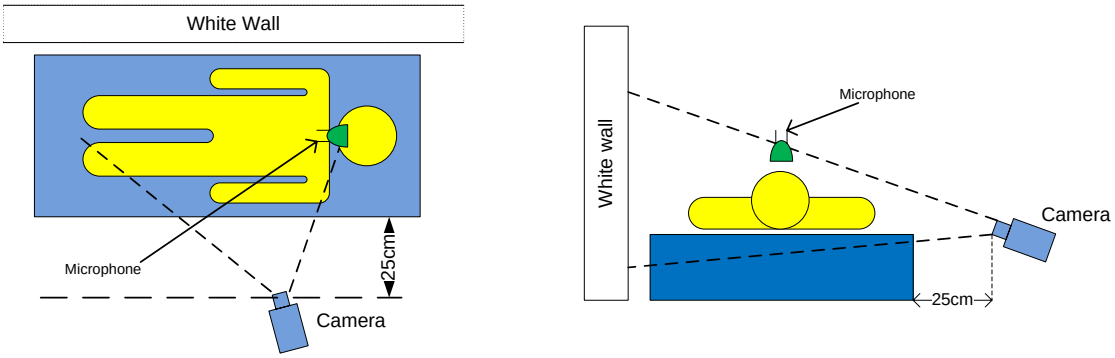

Figure 4.2: Diagram of the Ground Truth Data Acquisition system. The setup enables the chest movements to be clearly distinguished on the white background in the video file.

beginning and the end of apnea events and movements where extracted manually and entered in a different table. The event table is later compared to a similar table created from the outputs of the IBS. A similar table is created for movement detection. In this table, each detected movement is recorded and it is later used for calculating the accuracy in detection of movements on the bed by the IBS.

4.3 Temporal segmentation of events

The IFSM transforms events from time into pixel domain. The events are detected according to their features in the pixel domain. Eventually, temporal boundaries are derived from the pixel domain values. The correlation between events in time and their representations in the IFSM is shown in figures 3.8 and 3.10. Figure 3.8 shows the correlation between time series plots of two posture changes during the study and their representation in the IFSM. Since posture change induces large pressure changes on sensors, the bright region following the change is still present. The effect of filter transition time fades out as the cyclic respiration patterns fade in (figures 3.8 and 3.9.

Figure 3.10 contains two apnea events. The apnea events are shown by plotting 10 channels of data (top figure) and their corresponding frames in the IFSM. Here

temporal boundaries of the apnea events are marked by red arrows on the main diagonal of the figure (bottom). These boundaries are extracted as described in section 3.7. The pixel and frame numbers corresponding to each boundary is recorded individually as detailed in table 4.5 for example. Temporal boundaries of movement events are also recorded similarly as detailed in table 4.6.

Once the exact time of sleep events are extracted, assessment of the sleep quality could be done using simple statistical methods. Examples of such parameters are: apnea occurrence per hour of sleep, apnea duration per hour, movements per hour, average movement length, average respiration cycle duration, etc. The latter could be used for quantitative assessment of the respiration depth over time (profound versus shallow) , as could be seen in figure 4.4. In this figure, the respiration trend could be seen for subject "FK". As part of the experiment scenario, the subject begins to breathe more deeply for a few minutes and the depth of respiration starts to decrease again to shallow breathing. Figures similar to figure 4.4 can be used to investigate trends of changes in respiration depth over time. Transitions between shallow and profound breathing can also be seen in similar graphs.

4.4 Quantitative Performance Evaluation

Performance of the IBS needs to be evaluated to calculate the recall, precision and accuracy of the system. Recall and precision indicate how successful the system is in detecting the type of the event. Accuracy determines how accurate the IBS is in detecting the temporal boundaries of correctly detected events. The performance parameters mentioned above will be presented and discussed as follows.

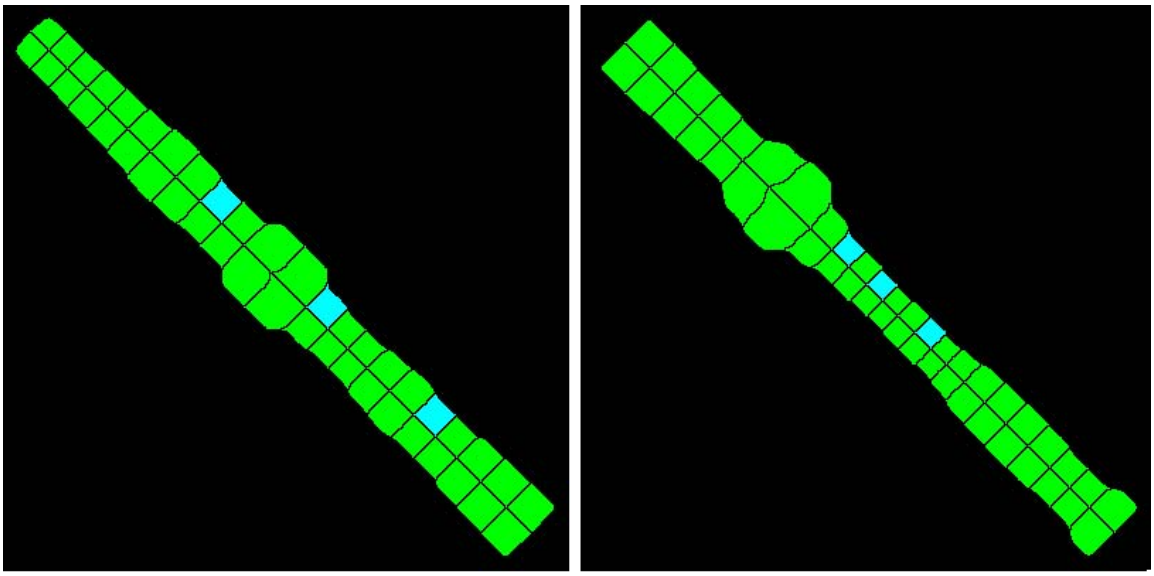

Figure 4.3: Transitions between shallow and profound breathing in the SIFSM. Larger squares represent profound respiration cycles. The transition in the respiration depth is derived from the changes in sizes of the squares.

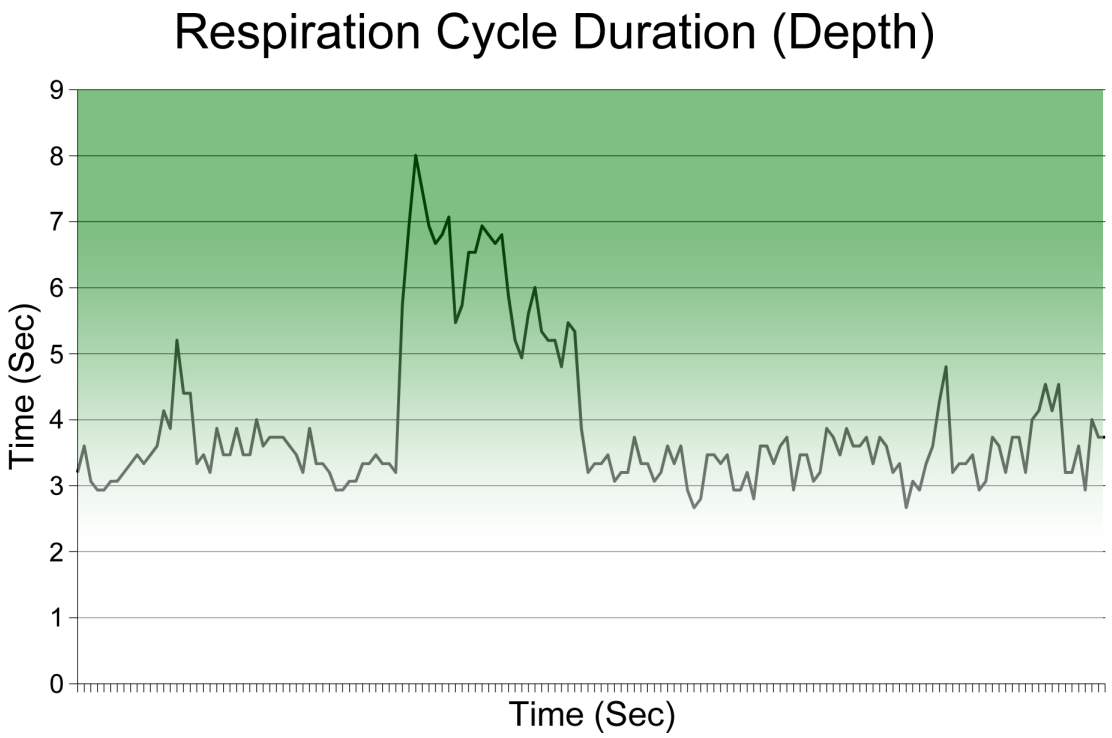

Figure 4.4: Evolution of respiration cycle duration over time. Darker regions indicate deeper respiration.

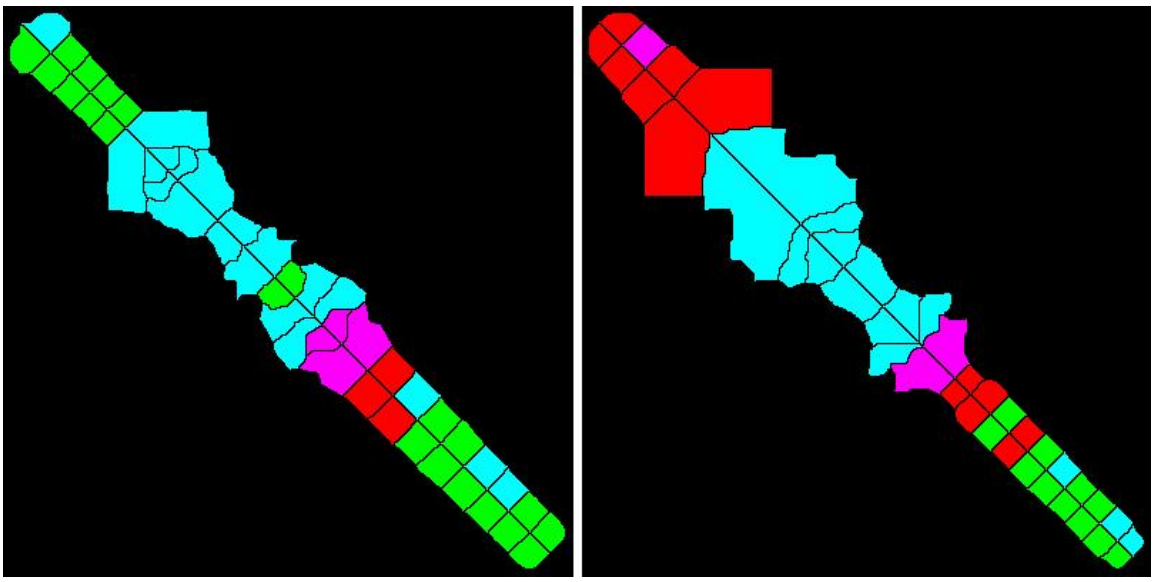

Figure 4.5: Apnea events are colored cyan. Left: sudden breath following an apnea is detected as movement. Right: panting preceding an apnea event and sudden breaths following it are detected as movement (purple and red).

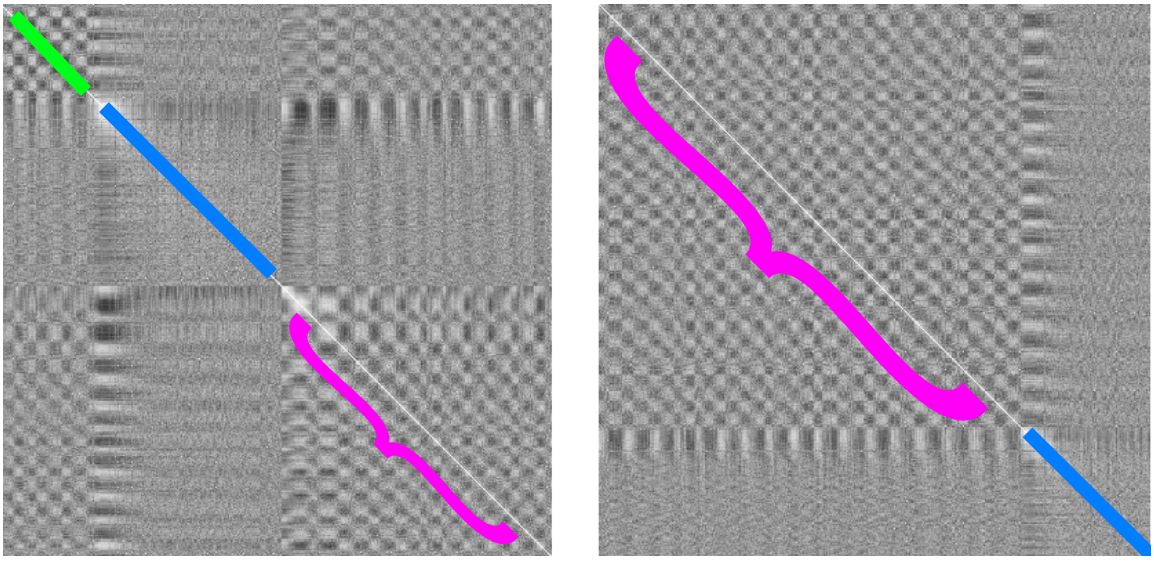

Figure 4.6: Left: The region marked green shows detected respiration cycles prior to an apnea. The Blue region is the apnea detected successfully followed by unclear respiration cycles (marked magenta) that could not be detected due to poor signal to noise ratio. Right: the proceeding frame of the SIFSM. The region marked magenta is the unclear respiration that is missed and causes the two apnea events (blue) merge into one.

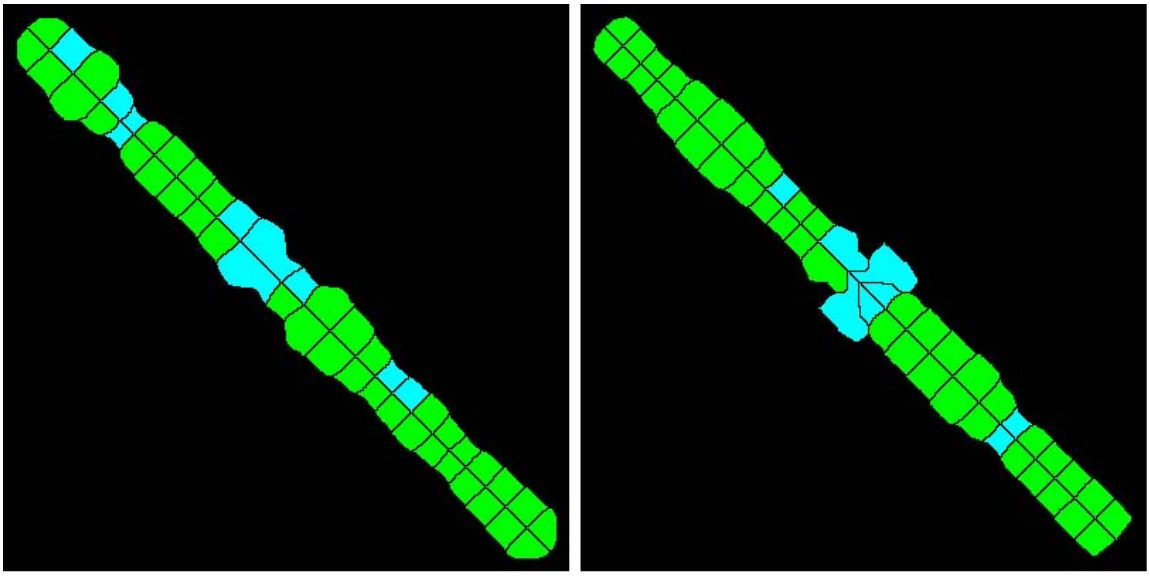

Figure 4.7: Small movements (usually slight limb movements) cause a disturbance in the SIFSM, but are not strong enough to be detected as movement. These regions are falsely detected and colored as apnea due to their shape.

4.4.1 Recall and Precision

The IBS is designed to detect three types of events, respiration, apnea and movement. How successful the system is in detecting the three types of events correctly is listed in table 4.3. This table indicates the recall and precision in detecting Apnea and Movement events per subject. The highest and lowest achieved recall and precision is 100 and 20 percent respectively. This high variance is explained by the limited number of events per subject in the database. Although the total number of simulated events are, for instance, 50 for apnea, there are only 5 events simulated per subject. This means, a single event counts 20% per subject. To summerize, 30 events have been identified correctly, 8 have been missed (detected as respiration) and 12 remaining events have been falsely marked as movement. Parameters affecting recall and precision are discussed thoroughly in section 4.5. Recall and Precision

are calculated as follows:

$$Recall = \frac{Correct Detection}{Correct \;\; Detections + Missed \;\; Events}, \tag{4.1}$$

$$Precision = \frac{Correct Detection}{Correct \;\; Detections + False \;\; Alarms}. \tag{4.2}$$

4.4.2 Accuracy

In order to evaluate the accuracy of the IBS, we manually marked events in the ground truth database that were detected correctly by the IBS. For each correct event the beginning and the end times are entered in a table. Temporal segmentation results from the IBS are also entered in a similar table. The two tables are then analyzed to calculate the error rate for each kind of event. The errors are calculated as:

$$E_{A_S}\ (sec)\ = T_{A_s} - t_{A_s}, \tag{4.3}$$

$$E_{A_E}\ (sec)\ = T_{A_e} - t_{A_e}, \tag{4.4}$$

$$E_{M_S}\ (sec)\ = T_{M_s} - t_{M_s}, \tag{4.5}$$

$$E_{M_E}\ (sec)\ = T_{M_e} - t_{M_e}, \tag{4.6}$$

where E_A and E_M denote the errors associated with detection of apnea and movement respectively. Subscripts S and E indicate the start and the end errors. In above equations, T_{A_s} denotes start time of the apnea event in the ground truth database and t_{A_s} denotes the start of the associating apnea detected by the IBS. Similarly, T_{A_e} and t_{A_e} denote end times in ground truth and IBS respectively. Beginning and end times of movements are denoted similarly.

The IBS was tested on our database of sleep pressure data. Results show that overall average error for detection of apnea events are 4.1 and 3.7 seconds for detection of the beginning and the end of apnea events as listed in table 4.5. The error for

detection of movements are detailed in tables 4.6. In these tables, negative error values correspond to instances when the IBS detects an event earlier than it happens in the ground truth. The average and standard deviation (STD) are calculated using the absolute value of the errors.

Subject	Resp as Apn	Resp as Mov	Apn Correct	Apn as Resp	Apn as Mov	Mov Correct	Mov as Resp	Mov as Apn	Apn Recall	Apn Precision	Mov Recal	Mov Precision
AM	2	0	3	2	0	2	0	1	**60.00%**	**100.00%**	**100.00%**	**66.67%**
ES	0	0	4	0	1	6	0	0	**100.00%**	**80.00%**	**100.00%**	**100.00%**
FK	0	0	1	0	4	6	0	1	**100.00%**	**20.00%**	**100.00%**	**85.71%**
KJ	0	0	2	2	1	3	0	3	**50.00%**	**66.67%**	**100.00%**	**50.00%**
MD	0	0	1	2	2	2	0	4	**33.33%**	**33.33%**	**100.00%**	**33.33%**
MG	0	0	2	1	2	2	0	4	**66.67%**	**50.00%**	**100.00%**	**33.33%**
NY	0	0	4	0	1	5	0	1	**100.00%**	**80.00%**	**100.00%**	**83.33%**
SM	0	1	3	1	1	1	3	1	**75.00%**	**75.00%**	**25.00%**	**50.00%**
SK	0	0	5	0	0	5	0	0	**100.00%**	**100.00%**	**100.00%**	**100.00%**
VT	1	0	5	0	0	4	0	2	**100.00%**	**100.00%**	**100.00%**	**66.67%**
Total	3	1	30	8	12	36	3	17				
Average									**78.50%**	**70.50%**	**92.50%**	**66.90%**
STD									**25.07%**	**28.24%**	**23.72%**	**25.03%**

Table 4.3: Precision and recall for detection of Apnea and Movement events listed per subject and in total.

4.5 Discussion

In a few cases, the recall and precision of detecting apnea are substantially lower than the others. This is due to interferences before and after the apneas. By investigating the ground truth videos, it could be seen that in cases where recall and precision are below 60%, subjects take a sudden deep breath upon hearing the auditory signals indicating the beginning and the end of apnea simulation. A sudden deep breath induces changes in the pressure that fall out of the statistical boundaries of valid respiration values (refer to section 3.3.1). Thus, a tick for movement is being kept in the memory for that moment, followed by a duration of, ideally, no noticeable change in the pressure (i.e. apnea). Upon hearing the apnea simulation end auditory signal, subjects take another deep breath or pant which triggers another movement event in the memory. The sequence of events described is identical to the sequence of events

in posture changes. Therefore, the probability that it is marked falsely as movement is noticeable. This sequence is shown in figure 4.5, right.

Furthermore, there are instances of missed (not detected) apnea events. The IBS detects the end of an apnea event by marking the beginning of the first respiration cycle following it. Although much less frequent than the previous case, this phenomenon happens when the respiration cycles proceeding an apnea event are not clear enough to be detected. Missed respiration cycles are caused by very poor signal to noise ratio. One parameter affecting the signal to noise ratio is the proximity of the pressure sensors to moving parts of the body. Since the spatial resolution of the sensors is quite low (i.e. 7.4 sensors per square foot), there are chances that only a few number of sensors pick up pressure fluctuations closely. Thus, considering the internal noises introduced by the electronics (refer to section 3.3), the signal to noise ratio would be lower than usual. The poor signal to noise ratio affects the detection of respiration cycles dramatically to the point that no cyclic respiration can be detected between two consecutive apnea events and until the subject changes the position or the posture on the bed. Therefore, two apnea events are detected as one, resulting in missed apnea events. This problem could be seen 8 times in the whole database. By increasing the spatial resolution of the sensors, there would be more sensors close to pressure fluctuations and a better signal to noise ratio is achieved. In addition, higher sampling rates provides more data over time and better filtering and signal processing could be performed prior to SIFSM formation. Thus, respiration cycles would be clearer and therefore, not missed. Figure 4.6 demonstrates the effect of low signal to noise ratio on detection of two consecutive apnea events. The effect of poor SNR in making the patterns unclear SNR could be seen in this figure comparing to other figures containing a frame of the SIFSM such as figures 3.7, 3.8 and 3.10.

There are three false alarms in apnea detection, when a normal respiration cycle is detected as apnea. There are two main causes for the false alarms in detection of

apnea. First, slight movements of the subject such as moving a hand or a foot. These small movements do not generate considerable changes in the pressure values, hence do not trigger a movement detection. However, they affect the cyclic pattern in the SIFSM and therefore result in an irregular shape after watershed segmentation as could be seen in figure 4.7.

The second cause of false alarms is again the signal to noise ratio. When the respiration patterns are not clear enough due to poor SNR, two or more cycles could be merged in the watershed segmentation step resulting in an irregular pattern, which is marked as apnea.

4.5.1 Sources of Error

There are two main sources of error in the system: movement events preceded by or preceding apnea events and very small movements. The effect of the first is shown in figure 4.5. As could be seen in this figure, there are red regions that indicate movements, attached to cyan regions representing an apnea. This is caused by oversensitivity of the movement detection algorithm that detects sudden deep breaths following or preceding simulated apnea events as movement. Note that red regions attached to apnea events have the shape of normal complete respiration cycles. The above mentioned error can be reduced by decreasing the sensitivity of the movement detection algorithm (increase the right hand side of the equation 3.4). This leads to an increase in the multiplicator before σ_i. However, this causes the contribution of the second error to increase. The second errors originates from slight movements that are not strong enough to be detected by the movement detection algorithm. On the other hand, these small movements change the shape of the region(s) in the IFSM. Deformed shapes are detected falsely as irregular breathing or apneas.

4.5.2 Hardware Limitations

There are certain limitations in the system that are imposed by the hardware. Limitations in the hardware affect the signal to noise ratio and subsequently the precision of detection. In addition, sweeping sampling rate makes conversion from sample number to time inaccurate. It has been investigated that the sampling rate drops dramatically as the acquisition duration increases. The average Sampling Rate for acquisitions of up to 18 minutes long where calculated 5.37 Hz using the following equation,

$$Sampling\ \ Rate\ \ (Hz) = \frac{Total\ \ number\ \ of\ \ samples}{Acquisition\ \ Duration\ \ (sec)}. \tag{4.7}$$

Using the same equation, the sampling rate for the 7 hour long acquisition has been calculated 3.6 Hz. This problem has been discussed with the manufacturer and it is under investigation.

4.6 Computation Time

The database was processed using a 2.40GHz personal computer equipped with 2GB of RAM. The computation time for each of the acquisitions is listed in table 4.4. In this table, the row indicated by "WN" corresponds to the whole night study and is not considered in the calculation of average and total computation times. "CSV2MAT" denotes the conversion of the raw pressure data to MATLAB data matrix. "Mov Detect" is the movement detection step as described in section 3.3.1."SIFSM", "ROI+Code" and "Log" refer to the calculation of the SIFSM, extraction of the region of interest and color coding, and creation of the sleep log steps respectively. Computation of the SIFSM is the most computationally intensive part of the system. Furthermore, movement detection contributes to the long processing time (figure 4.8).

Subject	CSV2MAT	Mov Detect	SIFSM	ROI+Code	Log	Total
WN	00:13:30.6	02:44:28.6	02:45:39.1	00:35:10.1	02:08:25.7	**08:27:14.12**
AM	00:00:54.1	00:06:15.1	00:09:28.5	00:01:48.6	00:00:32.0	**18:58.31**
ES	00:00:52.5	00:06:17.5	00:09:27.0	00:01:30.6	00:00:32.9	**18:40.47**
FK	00:00:49.9	00:06:19.2	00:09:39.8	00:01:57.7	00:00:31.6	**19:18.14**
KJ	00:00:48.7	00:06:11.0	00:09:32.3	00:01:44.3	00:00:31.1	**18:47.44**
MD	00:00:50.9	00:06:17.7	00:09:31.6	00:01:06.6	00:00:30.7	**18:17.59**
MG	00:00:51.7	00:06:20.5	00:09:28.6	00:01:16.4	00:00:31.2	**18:28.34**
NY	00:00:52.0	00:06:25.5	00:09:29.3	00:01:33.3	00:00:31.0	**18:50.95**
SM	00:00:46.2	00:06:23.3	00:09:26.1	00:01:00.8	00:00:31.1	**18:07.61**
SK	00:00:49.2	00:06:30.0	00:11:14.9	00:01:48.9	00:00:40.0	**21:02.94**
VT	00:00:49.9	00:06:20.3	00:09:28.5	00:01:34.6	00:00:29.2	**18:42.39**
Total	**00:08:25.1**	**01:03:20.0**	**01:36:46.5**	**00:15:21.8**	**00:05:20.8**	**03:09:14.19**
Average	**00:00:50.5**	**00:06:20.0**	**00:09:40.6**	**00:01:32.2**	**00:00:32.1**	**18:55.42**

Table 4.4: Processing time for each study in the database. The subject named "WN" refers to the whole night study and is not included in the average and total.

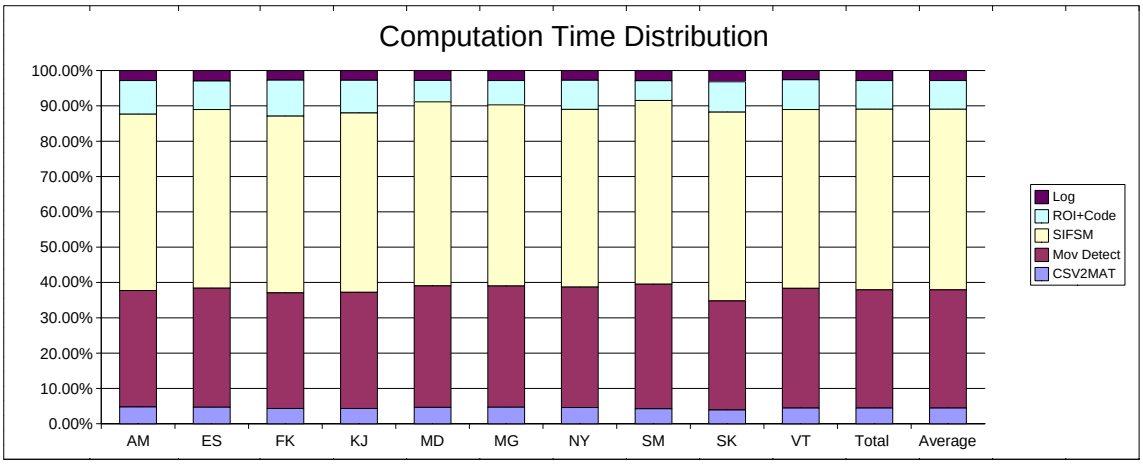

Figure 4.8: Distribution of computation time among various steps of the process. Almost half of the computation time consists of calculating the SIFSM. Detection of movements in the data is also a computationally intensive task.

Subject	E Mov Start F	E Mov Start P	E Mov End F	E Mov End P	T Mov Start F	T Mov Start P	T Mov End F	T Mov End P	Err S (Pixels)	Err E (Pixels)	Err S(Sec)	Err E (Sec)
AM	4	301	7	363	4	245	7	266	-56	-97	-10.43	-18.06
AM	12	304	15	340	12	308	15	323	4	-17	0.74	-3.17
AM	32	275	44	348	32	282	44	320	7	-28	1.3	-5.21
ES	2	320	4	355	2	330	4	370	10	15	1.86	2.79
ES	13	300	14	368	13	260	14	360	-40	-8	-7.45	-1.49
ES	21	320	24	354	21	340	24	365	20	11	3.72	2.05
ES	42	284	44	340	42	280	44	335	-4	-5	-0.74	-0.93
FK	12	338	15	360	12	340	15	358	2	-2	0.37	-0.37
KJ	23	295	24	339	23	230	24	334	-65	-5	-12.1	-0.93
KJ	41	287	43	371	41	310	43	360	23	-11	4.28	-2.05
MD	41	320	44	348	41	310	44	330	-10	-18	-1.86	-3.35
MG	20	344	34	331	20	390	34	321	46	-10	8.57	-1.86
MG	39	314	46	322	39	350	46	300	36	-22	6.7	-4.1
NY	2	303	5	346	2	308	5	330	5	-16	0.93	-2.98
NY	12	305	15	354	12	308	15	344	3	-10	0.56	-1.86
NY	32	299	33	377	32	280	33	377	-19	0	-3.54	0
NY	41	288	44	331	41	310	44	337	22	6	4.1	1.12
SM	3	293	7	274	3	271	7	227	-22	-47	-4.1	-8.75
SM	23	336	24	361	23	280	24	350	-56	-11	-10.43	-2.05
SM	41	289	44	352	41	327	44	330	38	-22	7.08	-4.1
SK	3	331	3	362	3	290	3	365	-41	3	-7.64	0.56
SK	12	314	13	350	12	320	13	353	6	3	1.12	0.56
SK	22	303	24	356	22	295	24	347	-8	-9	-1.49	-1.68
SK	31	325	31	380	31	356	33	346	31	66	5.77	12.29
SK	39	322	44	347	43	150	44	340	28	-7	5.21	-1.3
VT	2	309	6	378	2	313	6	340	4	-38	0.74	-7.08
VT	12	301	16	373	12	305	16	290	4	-83	0.74	-15.46
VT	20	306	24	358	20	315	24	345	9	-13	1.68	-2.42
VT	31	298	33	360	31	344	33	370	46	10	8.57	1.86
VT	40	323	43	359	40	330	43	370	7	11	1.3	2.05
Average									**22.4**	**20.13**	**4.17**	**3.75**
STD									**18.83**	**23.67**	**3.51**	**4.41**

Table 4.5: Apnea detection errors calculated using equations 4.3 and 4.4. In each case, columns starting with an "E" list values estimated by the IBS and those starting with a "T" indicate corresponding ground truth marking. Err S and Err E refer to errors in detection of the start and the end of the apnea event respectively. "P" and "F" postfixes indicate Pixel number and Frame number respectively. Conversion between pixel and time values are done using $Time\ (sec) = \frac{Pixel}{Sampling\ \ Rate}$, where Sampling Rate is assumed to remain constant at 5.3Hz.

Subject	E Mov Start F	E Mov Start P	E Mov End F	E Mov End P	T Mov Start F	T Mov Start P	T Mov End F	T Mov End P	Err S (Pixels)	Err E (Pixels)	Err S(Sec)	Err E (Sec)
AM	63	339	76	383	63	340	76	335	1	-48	0.19	-8.94
AM	81	354	83	366	81	358	86	314	4	98	0.74	18.25
ES	50	328	52	365	50	348	53	284	20	-31	3.72	-5.77
ES	64	333	66	378	64	343	66	370	10	-8	1.86	-1.49
ES	72	318	75	381	72	333	75	357	15	-24	2.79	-4.47
ES	78	357	78	375	78	350	78	378	-7	3	-1.3	0.56
ES	82	333	85	364	82	339	85	366	6	2	1.12	0.37
ES	92	325	95	360	92	338	95	362	13	2	2.42	0.37
FK	52	297	54	334	52	330	54	328	33	-6	6.15	-1.12
FK	55	345	55	364	55	346	55	368	1	4	0.19	0.74
FK	62	335	63	336	62	338	63	328	3	-8	0.56	-1.49
FK	74	321	77	363	74	310	77	357	-11	-6	-2.05	-1.12
FK	83	335	87	351	83	340	87	360	5	9	0.93	1.68
FK	94	310	100	364	94	313	100	260	3	-104	0.56	-19.37
KJ	71	345	75	346	71	370	75	364	25	18	4.66	3.35
KJ	82	311	85	357	82	320	85	358	9	1	1.68	0.19
KJ	92	316	95	350	92	320	95	345	4	-5	0.74	-0.93
MD	64	331	65	357	64	340	65	368	9	11	1.68	2.05
MD	72	306	75	357	72	328	75	350	22	-7	4.1	-1.3
MG	82	314	83	357	82	318	84	375	4	68	0.74	12.66
MG	90	366	95	364	91	380	95	345	64	-19	11.92	-3.54
NY	50	327	53	343	50	340	53	357	13	14	2.42	2.61
NY	64	309	66	339	64	310	66	355	1	16	0.19	2.98
NY	71	347	78	335	71	349	78	220	2	-115	0.37	-21.42
NY	82	298	86	352	82	305	86	330	7	-22	1.3	-4.1
NY	92	309	93	353	92	310	95	352	1	99	0.19	18.44
SM	47	318	47	350	47	310	47	352	-8	2	-1.49	0.37
SK	51	310	53	357	51	320	53	350	10	-7	1.86	-1.3
SK	66	280	66	365	66	270	66	376	-10	11	-1.86	2.05
SK	72	349	77	355	72	362	77	322	13	-33	2.42	-6.15
SK	82	350	86	333	82	370	86	346	20	13	3.72	2.42
SK	93	312	96	374	93	327	96	378	15	4	2.79	0.74
VT	51	294	51	369	51	300	51	390	6	21	1.12	3.91
VT	72	314	75	360	72	301	75	367	-13	7	-2.42	1.3
VT	82	320	85	367	82	315	85	358	-5	-9	-0.93	-1.68
VT	92	313	93	362	92	321	95	348	8	86	1.49	16.01
Average									**11.14**	**26.14**	**2.07**	**4.87**
STD									**11.66**	**33.32**	**2.17**	**6.21**

Table 4.6: Movement detection errors calculated using equations 4.5 and 4.6. In each case, columns starting with an "E" list values estimated by the IBS and those starting with a "T" indicate corresponding ground truth marking. Err S and Err E refer to errors in detection of the start and the end of the movement event respectively. "P" and "F" postfixes indicate Pixel number and Frame number respectively. Conversion between pixel and time values are done using $Time\ (sec) = \frac{Pixel}{Sampling\ \ Rate}$, where Sampling Rate is assumed to remain constant at 5.3Hz.

Chapter 5

Conclusion

5.1 Summary

This thesis presented a novel approach for detection of respiration and sleep disturbances from pressure signals using computer vision techniques. The Intelligent Bed Sensor (IBS) was proposed as an inexpensive home-based sleep monitoring alternative to sleep clinics. The IBS, as opposed to other similar techniques, is not invasive or intrusive. The only source of information used by the IBS is the pressure information recorded by the sensor sheet covering the mattress. The main contribution of the proposed approach is the application of computer vision techniques to improve upon signal processing techniques for detection of events in time series data. It also provides sleep information that was not extracted in previous works in the field, such as beginning and end of each respiration cycle, movement or apnea event. These features facilitate investigation of respiration statistics over extended periods of study. An example of such sleep statistics studies is quantitatively tracking the changes in the average depth of individual respiration cycles (shallow versus profound) over time, as shown in figure 4.4.

The IBS was tested using a database created following a designed experiment. The

experiment scenario was designed to contain 50 apnea and 50 movement events and posture changes as well as shallow/profound breathing and sleeping on lateral posture. The database created contains 50 apneas and 56 movement events in total. For the purpose of quantitative evaluation, a ground truth database has been created using a video camera and a microphone. The volunteers were captured by the camera and their respiration sounds were recorded by the microphone. The ground truth database was later used to mark events manually to be compared to the results from the IBS.

The pressure data was first filtered to enhance the overall dynamic range of the system. Movements are detected from sudden changes in time series pressure data, using statistical signal processing. The Inter-Frame Similarity Matrix (IFSM) is computed for a sliding window, taking 400 samples at a time and sliding 50 samples at each iteration. Each frame in the sequence of the IFSMs is segmented using the watershed segmentation algorithm. A region of interest (ROI) is extracted afterwards. Each region contained in the ROI is processed using region descriptors. Regions are classified as normal respiration, apnea or movement based on their shape and the *a priori* information, from the movement detection algorithm, about the movements that occurred.

5.2 Future Work

In order to overcome the problems discussed in section 4.5, two steps could be taken: improving the hardware and improving the pre-processing steps of the IBS. Using a bed sensor with a fixed sampling rate that is higher than the one used in this study will provide some redundancy in the information that could be used for denoising the signals. In addition, a fixed sampling rate will enhance the accuracy of conversion between pixel and time domains. Current bed sensor contains 144 pressure sensors.

This provides 7.4 sensors per square ft. Higher density of sensors will also help improve the signal to noise ratio.

Improvements in the preprocessing step could be achieved by applying statistical signal processing techniques, such as Principal Component Analysis (PCA) and Independent Components Analysis (ICA), prior to calculation of the SIFSM. Statistical signal processing techniques can be used to extract a desired number of active sources from all the sensors. Since the quality of the SIFMS is crucial for correct detection of repiration cycles and apneas, and it is closely related to the signal to noise ratio, using only active sources computed by ICA or most active components derived by PCA instead of all pressure sensors in the calculation of the IFSM will enhance the quality of the frames dramatically. This, particularly, addresses the problem when not many sensors are measuring the changes closely enough (refer to section 4.5).

Manually marking every respiration cycle and apnea event in the ground truth database manually is very time consuming. Therefore, in order to evaluate the IBS using larger databases, simultaneous Polysomnography is recommended. Nasal thermistor tubes could also be used for detection of apnea and respiration. They provide the fluctuations in the temperature of the nasal airways as the result of respiration. Nasal thermistors could be bought off the shelf along with their commercial software and hardware packages. The respiration and apnea results from the IBS could be compared to that or the thermistor tubes for evaluating the system. The IBS can also be installed in a sleep clinic to be benchmarked against the standard techniques.

Finally, the current database contains 3 hours of sleep information. A larger database that consists of more subjects is recommended for evaluation of the IBS. Furthermore, none of the subjects in our database had a known sleep-related breathing irregularity. Therefore, apnea events where only simulated. The IBS was tested once over night to confirm that it will function on larger datasets. However evaluating the IBS with real patients over multiple nights is recommended as future step.

Bibliography

[1] Alexandra Branzan Albu, Mehran Yazdi, and Robert Bergevin. Detection of cyclic human activities based on the morphological analysis of the inter-frame similarity matrix. *Real-Time Imaging*, 11(3):219–232, 6 2005.

[2] Najib T. Ayas, Stephen Pittman, Mary MacDonald, and David P. White. Assessment of a wrist-worn device in the detection of obstructive sleep apnea. *Sleep Medicine,*, 4(5):435–442, 9 2003.

[3] R. Balsree, A. Thawani, S. Gopalan, and V. Sridhar. Inter-frame similarity based video transcoding. *Multimedia, Seventh IEEE International Symposium on*, pages 6 pp.–, Dec. 2005.

[4] Bruce G. Bender, Susan B. Leung, and Donald Y. M. Leung. Actigraphy assessment of sleep disturbance in patients with atopic dermatitis: An objective life quality measure. *Journal of Allergy and Clinical Immunology,*, 111(3):598–602, 3 2003.

[5] Ann M. Berger, Lynne A. Farr, Brett R. Kuhn, Patricia Fischer, and Sangeeta Agrawal. Values of sleep/wake, activity/rest, circadian rhythms, and fatigue prior to adjuvant breast cancer chemotherapy. *Journal of Pain and Symptom Management,*, 33(4):398–409, 4 2007.

[6] Ann M. Berger, Kimberly K. Wielgus, Stacey Young-McCaughan, Patricia Fischer, Lynne Farr, and Kathryn A. Lee. Methodological challenges when using

actigraphy in research. *Journal of Pain and Symptom Management,*, In Press, Corrected Proof, 2007.

[7] A. Bieniek and A. Moga. An efficient watershed algorithm based on connected components. *Pattern Recognition*, 33(6):907–916, 6 2000.

[8] Andr Bleau and L. Joshua Leon. Watershed-based segmentation and region merging. *Computer Vision and Image Understanding*, 77(3):317–370, 3 2000.

[9] MH Bonnet and DL Arand. We are chronically sleep deprived. *sleep*, 18(10):908–11, December 1995.

[10] Pornvit Saksobhavivat Borko Furht. A fast content-based multimedia retrieval technique using compressed data. *Conference on Multimedia Storage and Archiving Systems III*, pages pp.561–57, 1998.

[11] Alexandra Branzan-Albu, Prabhat Kumar, Elaine Gallagher, and David Lockhorst. Monitoring sleep with computer vision techniques. *2nd International Conference on Technology and Aging*, May, 2007.

[12] Nan Bu, Naohiro Ueno, and Osamu Fukuda. Monitoring of respiration and heartbeat during sleep using a flexible piezoelectric film sensor and empirical mode decomposition. *Engineering in Medicine and Biology Society, 2007. EMBS 2007. 29th Annual International Conference of the IEEE*, pages 1362–1366, 22-26 Aug. 2007.

[13] D. Caggiano and S. Reisman. Respiration derived from the electrocardiogram: a quantitative comparison of three different methods. *Bioengineering Conference, 1996., Proceedings of the 1996 IEEE Twenty-Second Annual Northeast*, pages 103–104, Mar 1996.

[14] Yongjoon Chee, Jooman Han, Jaewoong Youn, and Kwangsuk Park. Air mattress sensor system with balancing tube for unconstrained measurement of respiration and heart beat movements. *Physiological Measurement*, 26(4):413–422, 2005.

[15] H Chen and Y Tank. Sleep loss impairs inspiratory muscle endurance. *Am Rev Respir Dis*, 140, 1989.

[16] M. Cooper and J. Foote. Scene boundary detection via video self-similarity analysis. *Image Processing, 2001. Proceedings. 2001 International Conference on*, 3:378–381 vol.3, 2001.

[17] R. Cutler and L.S. Davis. Robust real-time periodic motion detection, analysis, and applications. *Pattern Analysis and Machine Intelligence, IEEE Transactions on*, 22(8):781–796, Aug 2000.

[18] M. Drinnan, J. Allen, P. Langley, and A. Murray. Detection of sleep apnoea from frequency analysis of heart rate variability. *Computers in Cardiology 2000*, pages 259–262, 2000.

[19] M.G. Elfeky, W.G. Aref, and A.K. Elmagarmid. Warp: time warping for periodicity detection. *Data Mining, Fifth IEEE International Conference on*, pages 8 pp.–, Nov. 2005.

[20] C. A. Everson. Sustained sleep deprivation impairs host defense. *Am J Physiol Regul Integr Comp Physiol*, 265(5):R1148–1154, 1993.

[21] A. Figliola, O. A. Rosso, and E. Serrano. Detection of delay time between the alterations of cardiac rhythm and periodic breathing. *Physica A: Statistical Mechanics and its Applications,*, 327(1-2):174–179, 9/1 2003.

[22] AQ Fischer, BA Chaudhary, MA Taormina, and B Akhtar. Intracranial hemodynamics in sleep apnea. *Chest*, 102(5):1402–1406, 1992.

[23] Eduardo Gil, Jose Maria Vergara, and Pablo Laguna. Study of the relationship between pulse photopletismography amplitude decrease events and sleep apneas in children. *Engineering in Medicine and Biology Society, 2006. EMBS '06. 28th Annual International Conference of the IEEE*, pages 3887–3890, 30 2006-Sept. 3 2006.

[24] Rafael C. Gonzalez and Richard E. Woods. *Digital image processing.* Prentice-Hall, Reading, Mass. ; Don Mills, 2002.

[25] Suanne Goodrich and William C. Orr. An investigation of the validity of the lifeshirt in comparison to standard polysomnography in the detection of obstructive sleep apnea. *Sleep Medicine,*, In Press, Corrected Proof, 2008.

[26] Tadao Hori, Yoshio Sugita, Einosuke Koga, Shuichiro Shirakawa, Katuhiro Inoue, Sunao Uchida, Hiroo Kuwahara, Masako Kousaka, Toshinori Kobayashi, Yoichi Tsuji, Masayosi Terashima, Kazuhiko Fukuda, and Noriko Fukuda. Proposed supplements and amendments to 'A Manual of Standardized Terminology, Techniques and Scoring System for Sleep Stages of Human Subjects', the Rechtschaffen & Kales (1968) standard. *Psychiatry and Clinical Neurosciences*, 55(3):305–310, 2001.

[27] Sabine Horstmann, Christian W. Hess, Claudio Bassetti, Matthias Gugger, and Johannes Mathis. Sleepiness-related accidents in sleep apnea patients. *Sleep*, 23(3), March 2000.

[28] S. Iamratanakul, J. McNames, and B. Goldstein. Estimation of respiration from physiologic pressure signals. *Engineering in Medicine and Biology Society, 2003.*

Proceedings of the 25th Annual International Conference of the IEEE, 3:2734–2737 Vol.3, Sept. 2003.

[29] C Iber, S Ancoli-Isreal, AL Chesson, and SF Quan. The aasm manual for the scoring of sleep and associated events. *American Academy of Sleep Medicine, Westchester, IL*, 2007.

[30] Bernd Jahne. *Digital image processing : concepts, algorithms, and scientific applications*. Springer, Berlin ; New York, 1997.

[31] M.H. Jones, R. Goubran, and F. Knoefel. Identifying movement onset times for a bed-based pressure sensor array. *Medical Measurement and Applications, 2006. MeMea 2006. IEEE International Workshop on*, pages 111–114, 20-21 2006.

[32] E. Kaniusas, H. Pfutzner, and B. Saletu. Acoustical signal properties for cardiac/respiratory activity and apneas. *Biomedical Engineering, IEEE Transactions on*, 52(11):1812–1822, Nov. 2005.

[33] WD Killgore, DB Killgore, LM Day, C Li, GH Kamimori, and TJ Balkin. The effects of 53 hours of sleep deprivation on moral judgment. *Sleep*, 30(3), March 2007.

[34] Teng Li and In-So Kweon. A semantic region descriptor for local feature based image categorization. *Acoustics, Speech and Signal Processing, 2008. ICASSP 2008. IEEE International Conference on*, pages 1333–1336, 31 2008-April 4 2008.

[35] DAVID G. LOWE. Distinctive image features from scale-invariant keypoints. *International Journal of Computer Vision*, 60(2):91–110, November, 2004.

[36] Daniel lvarez, Roberto Hornero, Mara Garca, Flix del Campo, and Carlos Zamarrn. Improving diagnostic ability of blood oxygen saturation from overnight

pulse oximetry in obstructive sleep apnea detection by means of central tendency measure. *Artificial Intelligence in Medicine,*, 41(1):13–24, 9 2007.

[37] SE Martin, PK Wraith, IJ Deary, and NJ Douglas. The effect of nonvisible sleep fragmentation on daytime function. *Am. J. Respir. Crit. Care Med.*, 155(5):1596–1601, 1997.

[38] A. Matsubara and S. Tanaka. Unconstrained and noninvasive measurement of heartbeat and respiration using an acoustic sensor enclosed in an air pillow. *SICE 2003 Annual Conference*, 3:2875–2878 Vol.3, Aug. 2003.

[39] M.O. Mendez, D.D. Ruini, O.P. Villantieri, M. Matteucci, T. Penzel, S. Cerutti, and A.M. Bianchi. Detection of sleep apnea from surface ecg based on features extracted by an autoregressive model. *Engineering in Medicine and Biology Society, 2007. EMBS 2007. 29th Annual International Conference of the IEEE*, pages 6105–6108, Aug. 2007.

[40] MM Mitler, DF Dinges, and WC Dement. Sleep medicine, public policy, and public health. *Principles and Practice of Sleep Medicine*, 1994.

[41] K. Nakajima, Y. Matsumoto, and T. Tamura. A monitor for posture changes and respiration in bed using real time image sequence analysis. *Engineering in Medicine and Biology Society, 2000. Proceedings of the 22nd Annual International Conference of the IEEE*, 1:51–54 vol.1, 2000.

[42] K. Nakajima, A. Osa, and H. Miike. A method for measuring respiration and physical activity in bed by optical flow analysis. *Engineering in Medicine and Biology Society, 1997. Proceedings of the 19th Annual International Conference of the IEEE*, 5:2054–2057 vol.5, 1997.

[43] S.H. Nam, T.G. Yim, C.Y. Ryu, S.C. Shin, J.H. Kang, and S. Kim. The preliminary study of unobtrusive respiratory monitoring for e-health. *Engineering*

in Medicine and Biology Society, 2005. IEEE-EMBS 2005. 27th Annual International Conference of the, pages 3796–3798, 2005.

[44] Y. Nishida and T. Hori. Non-invasive and unrestrained monitoring of human respiratory system by sensorized environment. *Sensors, 2002. Proceedings of IEEE*, 1:705–710 vol.1, 2002.

[45] Y. Nishida, M. Takeda, T. Mori, H. Mizoguchi, and T. Sato. Monitoring patient respiration and posture using human symbiosis system. *Intelligent Robots and Systems, 1997. IROS '97., Proceedings of the 1997 IEEE/RSJ International Conference on*, 2:632–639 vol.2, Sep 1997.

[46] S. M. O'Malley, J. F. Granada, S. Carlier, M. Naghavi, and I. A Kakadiaris. Image-based gating of intravascular ultrasound pullback sequences. *Information Technology in Biomedicine, IEEE Transactions on*, 12(3):299–306, May 2008.

[47] Vctor Osma-Ruiz, Juan I. Godino-Llorente, Nicols Senz-Lechn, and Pedro Gmez-Vilda. An improved watershed algorithm based on efficient computation of shortest paths. *Pattern Recognition*, 40(3):1078–1090, 3 2007.

[48] Allan I. Pack, Greg Maislin, Bethany Staley, Frances M. Pack, William C. Rogers, Charles F. P. George, and David F. Dinges. Impaired Performance in Commercial Drivers: Role of Sleep Apnea and Short Sleep Duration. *Am. J. Respir. Crit. Care Med.*, 174(4):446–454, 2006.

[49] Ya-Ti Peng, Ching-Yung Lin, Ming-Ting Sun, and C.A. Landis. Multimodality sensor system for long-term sleep quality monitoring. *Biomedical Circuits and Systems, IEEE Transactions on*, 1(3):217–227, Sept. 2007.

[50] T. Penzel, K. Kesper, T. Ploch, H.F. Becker, and C. Vogelmeier. Ambulatory recording of sleep apnea using peripheral arterial tonometry. *Engineering*

in Medicine and Biology Society, 2004. IEMBS '04. 26th Annual International Conference of the IEEE, 2:3856–3859, Sept. 2004.

[51] O. Postolache, P.S. Girao, G. Postolache, and M. Pereira. Vital signs monitoring system based on emfi sensors and wavelet analysis. *Instrumentation and Measurement Technology Conference Proceedings, 2007 IEEE*, pages 1–4, May 2007.

[52] M.I. Restrepo, S. Bhandari, and Taikang Ning. Classification of respiration episodes using fuzzy logic. *Bioengineering Conference, 2006. Proceedings of the IEEE 32nd Annual Northeast*, pages 133–134, 2006.

[53] MR Risser, JC Ware, and FG Freeman. Driving simulation with eeg monitoring in normal and obstructive sleep apnea patients. *Sleep*, 23(3), May 2000.

[54] Avi Sadeh and Christine Acebo. The role of actigraphy in sleep medicine. *Sleep Medicine Reviews,*, 6(2):113–124, 5 2002.

[55] Avi Sadeh, Christine Acebo, R. Seifer, Semra Aytur, and Mary A. Carskadon. Activity-based assessment of sleep-wake patterns during the 1st year of life. *Infant Behavior and Development,*, 18(3):329–337, 0 1995.

[56] John I. Salisbury and Ying Sun. Rapid screening test for sleep apnea using a nonlinear and nonstationary signal processing technique. *Medical Engineering & Physics,*, 29(3):336–343, 4 2007.

[57] N. Sezgin, G. Kirbas, and M. Akin. The correlation analysis between airflow and oxygen saturation in obstructive sleep apnea events using correlation function. *Signal Processing and Communications Applications, 2007. SIU 2007. IEEE 15th*, pages 1–5, June 2007.

[58] T.T. Shannon, J. McNames, M.S. Ellenby, and B. Goldstein. Modeling respiration from blood pressure waveform signals: an independent component approach. *[Engineering in Medicine and Biology, 2002. 24th Annual Conference and the Annual Fall Meeting of the Biomedical Engineering Society] EMBS/BMES Conference, 2002. Proceedings of the Second Joint*, 1:200–201 vol.1, 2002.

[59] Karine Spiegel, Esra Tasali, Plamen Penev, and Eve Van Cauter. Brief Communication: Sleep Curtailment in Healthy Young Men Is Associated with Decreased Leptin Levels, Elevated Ghrelin Levels, and Increased Hunger and Appetite. *Ann Intern Med*, 141(11):846–850, 2004.

[60] Tara W. Strine and Daniel P. Chapman. Associations of frequent sleep insufficiency with health-related quality of life and health behaviors. *Sleep Medicine*, 6(1):23–27, 1 2005.

[61] KP Strohl and S Redline. Recognition of obstructive sleep apnea. *Am. J. Respir. Crit. Care Med.*, 154(2):279–289, 1996.

[62] S.R. Suhas, K. Behbehani, S. Vijendra, J.R. Burk, and E.A. Lucas. Time domain analysis of r-wave attenuation envelope for sleep apnea detection. *Engineering in Medicine and Biology Society, 2004. IEMBS '04. 26th Annual International Conference of the IEEE*, 2:3885–3888 Vol.6, Sept. 2004.

[63] S.R. Suhas, S. Vijendra, J.R. Burk, E.R. Lucas, and K. Behbehani. Spectral analysis of r wave attenuation and heart rate variability for detection of cheyne stokes breathing. *Engineering in Medicine and Biology Society, 2005. IEEE-EMBS 2005. 27th Annual International Conference of the*, pages 1216–1219, 2005.

[64] K. Toshima, T. Watanabe, Y. Kaneko, T. Maesako, and K. Takahashi. Diaphragm-type optical fiber pressure sensor with a sleeve for fiber insertion.

Micromechatronics and Human Science, 2003. MHS 2003. Proceedings of 2003 International Symposium on, pages 171–174, Oct. 2003.

[65] M. Uchida, Wenxi Chen, T. Nemoto, K. Kitamura, Y. Kanemitsu, and Daming Wei. An ICA approach to reject noise from pressure changes of pillow. *Computer and Information Technology, 2004. CIT '04. The Fourth International Conference on*, pages 916–921, 14-16 Sept. 2004.

[66] P. Varady and S. Bongar. Detection of airway obstruction and sleep apnea by analyzing the phase relation of respiration movement signals. *Instrumentation and Measurement Technology Conference, 2001. IMTC 2001. Proceedings of the 18th IEEE*, 1:185–190 vol.1, May 2001.

[67] P. Varady, S. Bongar, and Z. Benyo. Detection of airway obstructions and sleep apnea by analyzing the phase relation of respiration movement signals. *Instrumentation and Measurement, IEEE Transactions on*, 52(1):2–6, Feb 2003.

[68] P. Varady, T. Micsik, S. Benedek, and Z. Benyo. A novel method for the detection of apnea and hypopnea events in respiration signals. *Biomedical Engineering, IEEE Transactions on*, 49(9):936–942, Sep 2002.

[69] A. N. Vgontzas, E. Zoumakis, E. O. Bixler, H.-M. Lin, H. Follett, A. Kales, and G. P. Chrousos. Adverse Effects of Modest Sleep Restriction on Sleepiness, Performance, and Inflammatory Cytokines. *J Clin Endocrinol Metab*, 89(5):2119–2126, 2004.

[70] K. Watanabe, T. Watanabe, H. Watanabe, H. Ando, T. Ishikawa, and K. Kobayashi. Noninvasive measurement of heartbeat, respiration, snoring and body movements of a subject in bed via a pneumatic method. *Biomedical Engineering, IEEE Transactions on*, 52(12):2100–2107, Dec. 2005.

[71] DP White, NJ Douglas, and CK Pickett. Sleep deprivation and control of ventilation. *Am Rev Respir Dis*, 128, 1983.

[72] Robert Wolk, Apoor S. Gami, Arturo Garcia-Touchard, and Virend K. Somers. Sleep and cardiovascular disease. *Current Problems in Cardiology,*, 30(12):625–662, 12 2005.

[73] Robert Wolk, Tomas Kara, and Virend K. Somers. Sleep-Disordered Breathing and Cardiovascular Disease. *Circulation*, 108(1):9–12, 2003.

[74] W.J. Yi and K.S. Park. Derivation of respiration from ecg measured without subject's awareness using wavelet transform. *[Engineering in Medicine and Biology, 2002. 24th Annual Conference and the Annual Fall Meeting of the Biomedical Engineering Society] EMBS/BMES Conference, 2002. Proceedings of the Second Joint*, 1:130–131 vol.1, 2002.

[75] T Young, J Blustein, L Finn, and M Palta. Sleep-disordered breathing and motor vehicle accidents in a population-based sample of employed adults. *sleep*, August 1997.

[76] X. Zhu, W. Chen, T. Nemoto, Y. Kanemitsu, K.-I. Kitamura, K.-I. Yamakoshi, and D. Wei. Real-time monitoring of respiration rhythm and pulse rate during sleep. *Biomedical Engineering, IEEE Transactions on*, 53(12):2553–2563, Dec. 2006.